





Bacterial flavoprotein monooxygenase YxeK salvages toxic S-(2-succino)-adducts via oxygenolytic C-S bond cleavage

Arne Matthews¹, Julia Schönfelder², Simon Lagies³ (i), Erik Schleicher², Bernd Kammerer^{3,4}, Holly R. Ellis⁵, Frederick Stull⁶ and Robin Teufel¹ (i)

- 1 Faculty of Biology, University of Freiburg, Germany
- 2 Institute of Physical Chemistry, University of Freiburg, Germany
- 3 Institute of Organic Chemistry, University of Freiburg, Germany
- 4 BIOSS Center for Biological Signaling Studies, University of Freiburg, Germany
- 5 Brody School of Medicine, East Carolina University, Greenville, NC, USA
- 6 Department of Chemistry, Western Michigan University, Kalamazoo, MI, USA

Keywords

flavin-dependent monooxygenase; flavin-N5peroxide; oncometabolite; oxidoreductase; oxygenolytic bond cleavage

Correspondence

R. Teufel, Faculty of Biology, University of Freiburg, Schänzlestrasse 1, 79104 Freiburg, Germany

Tel: +49-761-97201

E-mail: robin.teufel@zbsa.uni-freiburg.de

(Received 30 April 2021, revised 18 August 2021, accepted 9 September 2021)

doi:10.1111/febs.16193

Thiol-containing nucleophiles such as cysteine react spontaneously with the citric acid cycle intermediate fumarate to form S-(2-succino)-adducts. In Bacillus subtilis, a salvaging pathway encoded by the yxe operon has recently been identified for the detoxification and exploitation of these compounds as sulfur sources. This route involves acetylation of S-(2succino)cysteine to N-acetyl-2-succinocysteine, which is presumably converted to oxaloacetate and N-acetylcysteine, before a final deacetylation step affords cysteine. The critical oxidative cleavage of the C-S bond of N-acetyl-S-(2-succino)cysteine was proposed to depend on the predicted flavoprotein monooxygenase YxeK. Here, we characterize YxeK and verify its role in S-(2-succino)-adduct detoxification and sulfur metabolism. Detailed biochemical and mechanistic investigation of YxeK including ¹⁸O-isotope-labeling experiments, homology modeling, substrate specificity tests, site-directed mutagenesis, and (pre-)steady-state kinetics provides insight into the enzyme's mechanism of action, which may involve a noncanonical flavin-N5-peroxide species for C-S oxygenolysis.

Introduction

The redox-active enzyme cofactors flavin mononucleotide (FMN) and flavin-adenine dinucleotide (FAD) derive from riboflavin (vitamin B2) and are exploited in nature for the catalysis of numerous fundamental reactions [1–8]. Both FMN and FAD share the isoal-loxazine ring system with the reactive N5-C4a locus that is central to their reactivity, for example, for

uptake/release of electrons and as a site for covalent adduct formation with substrates or dioxygen (O₂) [1,6]. Flavoprotein monooxygenases (FPMOs) in particular are capable of transferring one molecule of O₂ to an organic substrate and enable reactions such as (aromatic) hydroxylation, Baeyer–Villiger oxidation, or carbon-heteroatom bond cleavage [1,4,5,8]. In general,

Abbreviations

2SC, S-(2-succino)-L-cysteine; DAC, N,N'-diacetylcystine; DNPH, 2,4-dinitrophenylhydrazine; DTNB, 5,5'-dithiobis-(2-nitrobenzoic acid); EDC, 1-(3-dimethylaminopropyl)-3-ethylcarbodiimide; Fl_{C4aOO(H)}, flavin-C4a-(hydro)peroxide; Fl_{N5OO(H)}, flavin-N5-(hydro)peroxide; Fl_{ox}, oxidized flavin; Fl_{red}, reduced flavin; Fl_{SQ}, flavin semiquinone; FMN, flavin mononucleotide; FPMO, flavoprotein monooxygenase; Fre, flavin reductase; GSS, S-succinylglutathione; HPLC, high-performance liquid chromatography; HRMS, high-resolution mass spectrometry; IS, internal standard; MRM, multiple reaction monitoring; NAC, N-acetyl-L-cysteine; NAC2SC, N-acetyl-S-(2-succino)-L-cysteine; oBHA, O-benzylhydroxylamine hydrochloride; RP-UPLC, reversed-phase ultraperformance liquid chromatography; SEC, size-exclusion chromatography.

FPMOs require an electron donor (typically NAD(P) H) for reduction of the oxidized quinonic flavin cofactor (Flox) to the hydroquinone form (Flred), which then reacts with O2. This process most likely involves single electron transfer from Fl_{red} to O₂, giving rise to transient flavin semiquinone (Fl_{SO}) and superoxide radical species that collapse to a covalent flavin-oxygen adduct. The regioselectivity of flavin oxygenation and functionalization is hereby likely determined by the geometry of approach of O₂ to the cofactor as well as the protonation state and electron configuration of the Fl_{SO} species that can be controlled by the protein matrix [1,6,9-13] and are thus pivotal for FPMO functionality [1,4,10,11]. Typically, FPMOs form transient flavin-C4a-(hydro)peroxide (Fl_{C4aOO(H)}) adducts, which serve as reactive oxygen transferring species [6,9,14]. Alternatively, the recently reported N5-oxygen adducts in the form of the flavin-N5-(hydro)peroxide (Fl_{N5OO} (H) [12,15] or flavin-N5-oxide (Fl_{N5O}) [11,15–18] are generated, both of which are chemically distinct in reactivity compared to the $Fl_{C4aOO(H)}$ species [1].

As of yet, FPMOs are classified based on the flavin reduction mode as well as their structural and functional features, which do not include oxygenation chemistry [1,5,6,8]. For example, group C FPMOs are FMNdependent two-component systems relying on separate NAD(P)H-dependent flavin reductases to provide Fl_{red} for the catalytic FPMO constituents that feature a TIMbarrel protein fold [5,19]. Remarkably, both N5- and C4a-oxygenated FMN cofactors are seemingly employed within this group [1], as illustrated by the prototypal Fl_{C4aOO}-dependent luciferase LuxA enabling bacterial bioluminescence [20] and the Fl_{N5OO}-dependent RutA [1,12], which catalyzes the key step of pyrimidine catabolism in Escherichia coli [18,21]. While there are still open questions how FMPOs control their reaction with O₂, a recently reported 'O2 reactivity motif' proved critical for N5-oxygenation in RutA and seemed more widespread in group C FPMOs [1,12]. The residues that are part of this motif participate in formation of a distinct O₂ reaction pocket adjacent to N5 of FMN and most likely steer the regiospecific cofactor oxygenation. As expected, this motif is missing in LuxA that features a starkly different protein microenvironment around the FMN cofactor [1,12]. Group C FPMOs that share the RutA-like O_2 reactivity motif [12] are often involved in the degradation of (man-made) environmental pollutants such as HcbA1 from Nocardioides sp. strain PD653 [22-24], DszA from Rhodococcus erythropolis [25,26] (or its functional homologue BdsA from Bacillus subtilis WU-S2B [27]), and EmoA from Chelativorans sp. BNC1 [28] that process hexachlorobenzene [12,22–24], dibenzothiophene sulfone [12,25,26], and ethylenediaminetetraacetate (EDTA),

respectively [28]. The formed Fl_{N5OO} of pyrimidine oxyhexachlorobenzene genase RutA, dehalogenasemonooxygenase HcbA1, and dibenzothiophene sulfone monooxygenase DszA then enables carbon-heteroatom bond (C-N, C-Cl, C-S) cleaving oxygenations that proceed via the unusual redox-neutral (nonoxidative) transfer of an [OH] from the Fl_{N5OO} to the substrates; reactions that resemble hydrolysis and afford Fl_{N5O} as a by-product [1,12]. In contrast, other related enzymes such as EDTA monooxygenase EmoA [28] and alkanesulfonate monooxygenase SsuD from E. coli [29] apparently mediate oxidative carbon-heteroatom bond cleavage reactions.

Recently, the putative group C FMPO YxeK from Bacillus subtilis 168 was reported [30] that also features a RutA-like O₂ reactivity motif [12], thus pointing toward the possible involvement of flavin-N5-oxygen adducts in its catalytic cycle. YxeK is encoded by a gene cluster required for the detoxification and salvaging of diasteromeric S-(2-succino)cysteine (2SC, 1), which is first converted by acetyltransferase YxeL to N-acetyl-(2-succino)cysteine (NAC2SC, 2). Next, YxeK presumably cleaves 2 into oxaloacetate (3) and Nacetyl-L-cysteine (4), which is further broken down by deacetylase YxeP to L-cysteine (5) and acetate (6) as the final products (Fig. 1) [30]. Compound 1 in turn arises from the spontaneous Michael addition of the soft nucleophile 5 to the electrophilic citric acid cycle intermediate fumarate and is expectedly found in a wide range of organisms including humans. Moreover, 1 accumulates in some cancer types and is thus considered an oncometabolite [31]. Similar to 5, the abundant cellular antioxidant glutathione (GSH) can become succinated by reacting with fumarate, which leads to oxidative stress and cellular aging [32]. In addition, cysteinyl residues of proteins are prone to undergo such succination, resulting in their covalent modification and thus potential functional impairment, as shown, for example, for aconitase [33], actin/tubulin [34,35], or glyceraldehyde-3-phosphate dehydrogenase [36]. In this study, we set out to verify the role of YxeK in the first reported pathway for salvaging of 1 in B. subtilis and characterize the enzyme features, substrate scope, and proposed oxygenative carbonsulfur bond cleavage reaction in more detail.

Results and Discussion

Flavoprotein monooxygenase YxeK oxidatively cleaves *N*-acetyl-*S*-(2-succino)-L-cysteine

To investigate the proposed role of YxeK in 1 metabolism and gain insight into the enzyme mechanism, the

Fig. 1. Proposed pathway for detoxification and breakdown of S-(2-succino)-L-cysteine (2SC, 1) in *B. subtilis* through enzymes encoded by the *yxeKLMNOPQ* operon [30]. Cysteine succination occurs spontaneously through Michael addition of L-cysteine to fumarate. N-acetylation by YxeL (green) then produces diastereomeric *N*-acetyl-S-(2-succino)-L-cysteine (NAC2SC, 2). Based on metabolic profiling experiments, the FPMO YxeK (orange) may then convert 2 to oxaloacetate (3) and *N*-acetyl-L-cysteine (NAC, 4). Deacetylation of 4 by YxeP (blue) or other redundant NAC deacetylases finally yields L-cysteine (5) and acetate (6). The genes *yxeMNO* may encode a transporter for sulfur-containing compounds. YxeQ is a protein of unknown function, which was not required for growth on 1. The length of the scale bar represents one kilobase.

yxeK gene was first amplified from Bacillus subtilis 168, cloned into pET28b for expression with an Nterminal His-tag, and produced in Escherichia coli BL21 (DE3). Following the protein purification via Ni²⁺ affinity and size-exclusion chromatography (SEC), YxeK was obtained at apparent homogeneity and formed dimers as determined by analytical SEC (Fig. S1a,b). Previous phylogenetic analysis placed YxeK in the group C of FMN-dependent twocomponent FPMOs [12]. Similar to some other reported group C FPMOs [19], in silico genome analysis did not reveal any nearby genes that could encode a putative flavin reductase for YxeK. As oxygenase constituents typically do not show strict specificities for their interaction partner, the E. coli flavin reductase Fre [37] was heterologously produced and used for the following experiments. As anticipated, chemically synthesized 2 (produced via a previously reported one step synthesis from 4 and fumarate [30]) was consumed by YxeK in the presence of both Fre and NADH but not in a control reaction lacking YxeK (Fig. 2). To analyze the YxeK / Fre-NADH catalyzed reaction and presumed formation of 3, derivatization with 2,4-dinitrophenylhydrazine (DNPH) was required prior to RP-UPLC and HRMS analysis due to poor ionization and interaction of 3 with reversed-phase (RP) chromatographic stationary phases [38,39]. Indeed, YxeK-dependent DNPH-3 formation could be demonstrated by UPLC (absorption detection at

360 nm) (Fig. 2A,B) and confirmed by UPLC-HRMS analysis, which additionally showed the formation of N,N'-diacetylcystine (7) arising from the dimerization of **4** (which cannot be detected under these conditions) (Fig. 2C–E).

Next, UPLC-HRMS analysis of the YxeK-catalyzed reaction was conducted in the presence of 16O2 and ¹⁸O₂ to investigate whether YxeK functions as a monooxygenase. For the detection of ¹⁸O incorporation into 3, a different derivatization strategy had to be pursued that did not involve the substitution of the enzymatically introduced oxygen. For that, the ketone in 3 was first transformed to the less reactive tertiary alcohol by condensing 3 with acetyl-CoA to citrate (8) using citrate synthase. Then, the terminal carboxyl groups of 8 were derivatized with Obenzylhydroxylamine hydrochloride (oBHA) and 1-(3dimethylaminopropyl)-3-ethylcarbodiimide (EDC) to generate 9 (Fig. 3A). Indeed, in the presence of ¹⁸O₂, 9 derived from YxeK-produced 3 carried a single ¹⁸Oisotope label, thus verifying the monooxygenase functionality of YxeK and confirming the anticipated oxidative C-S bond cleavage reaction required for the processing of 1 (Fig. 3B,C). Notably, this reaction is different from the RutA-like Fl_{N5OO}-dependent redoxneutral 'pseudo-hydrolysis', as 2 is oxidatively cleaved by YxeK via the more typical formal transfer of an [OH]⁺ (rather than [OH]⁻) similar to EmoA and SsuD. A closer inspection of the proposed catalyzed reactions

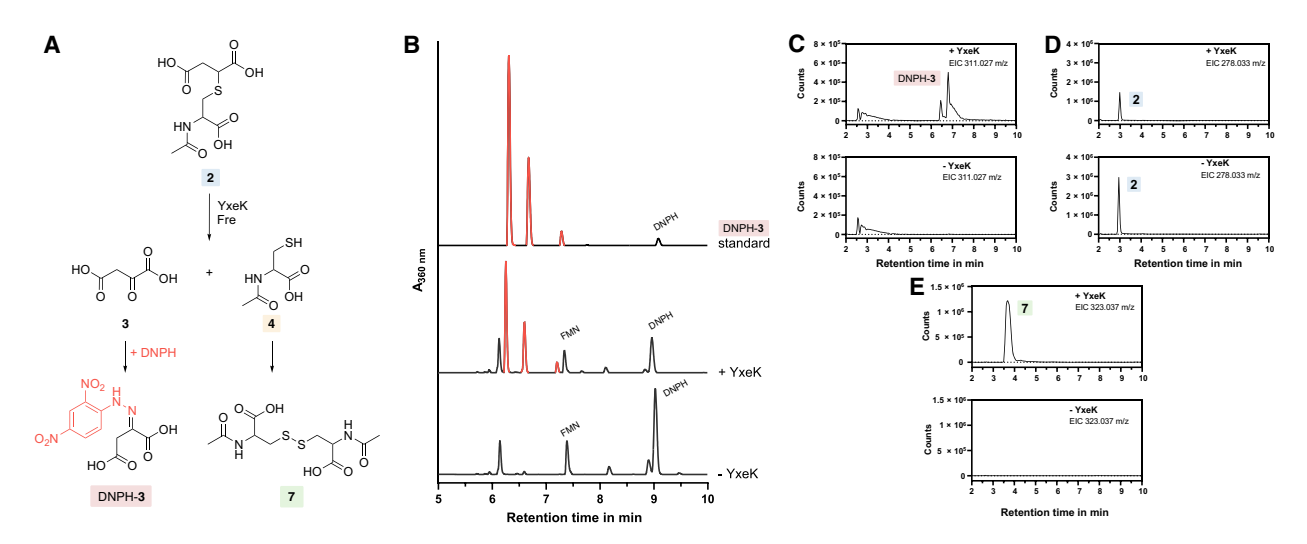


Fig. 2. Characterization of the YxeK / Fre-NADH catalyzed reaction. (A) Structures of substrate and products. (B) RP-UPLC analysis (absorption at 360 nm) of enzymatic assays showing production of **3** by YxeK and Fre-NADH that is derivatized with DNPH (middle lane, DNPH-**3** highlighted in red). The bottom lane shows the control without YxeK, and the top lane shows a standard of **3** derivatized with DNPH. Note that the smaller product peaks (also in red) likely arise from spontaneous decarboxylation of DNPH-**3**. (C-F) UPLC-HRMS analysis of the YxeK reaction products (top lanes) and control reactions (lower lanes). Shown are the extracted ion chromatograms (EICs) of DNPH-**3** (C), substrate **2** (D), *N*,*N'*-diacetylcystine **7** (E). Three independent biological replicates (*n* = 3) were analyzed and a representative data set is shown.

of (partially) characterized group C FPMOs (which feature a RutA-like O₂ reactivity motif) showed that most members seemingly mediate oxidative (YxeK, NtaA, EmoA, DmoA, SfnG, SsuD, and MsuD) rather than nonoxidative (RutA, HcbA1, DszA) oxygenation reactions (Fig. S2).

YxeK substrate specificity and steady-state kinetics

In addition to cellular cysteine, glutathione is another dominant metabolite that readily reacts with fumarate to S-succinylglutathione (10, GSS). To investigate the substrate specificity of YxeK, 10 was chemically synthesized and purified for in vitro assays. Compound 10, as well as the commercially available 2succinocysteine (1), were tested using Ellman's assay based on the reaction of 5,5'-dithiobis-(2-nitrobenzoic acid) (DTNB) with free thiol groups formed upon substrate cleavage. The produced TNB²⁻ is stoichiometric to the amount of released thiol groups, allowing product quantification through measuring the absorbance at 412 nm. YxeK converted the natural substrate 2 with an apparent maximal turnover number (k_{cat}) of $4.4 \pm 0.2 \text{ s}^{-1}$ and a K_M value of 92 ± 16 µM, while both 10 and 1 were also accepted as substrates for oxidative C-S bond cleavage at relative activities of 0.6% and 0.2% compared to the k_{cat} value with 2, respectively (Fig. 4A-C). Overall, these results clearly show that $\mathbf{2}$ is the preferred substrate of YxeK. However, formation of Fl_{N5O} was not observed as Fl_{ox} was the only detectable flavin intermediate through UPLC-HRMS analysis (though the Fl_{N5O} is typically sufficiently stable for detection by UPLC-HRMS in contrast to the labile flavin-peroxy adducts), when YxeK was incubated with natural substrate $\mathbf{2}$ or noncleavable analogs *N*-acetyl-L-glutamic acid ($\mathbf{12}$) and γ -carboxyl-DL-glutamic acid ($\mathbf{13}$) (Fig. 5A–D). It is also noteworthy that YxeK may work more efficiently *in vivo* when interacting with its native partner flavin reductase rather than Fre, as previously reported for EDTA monooxygenase EmoA and reductase EmoB [28].

Homology modeling and biochemical studies support a RutA-like O₂ activation for YxeK

YxeK was then compared to previously characterized and closely related group C FPMOs that share the RutA-like O₂ reactivity motif. For some of these enzymes, mobile, lid-like loops were identified that are important for catalysis, for example, in EDTA monooxygenase EmoA [28] and alkanesulfonate monooxygenase SsuD [40,41]. Only for EmoA, however, distinct structures for both open and closed loop conformations were solved, whereas in the protein structures of SsuD, the distantly related RutA and others, these loop regions were open or remained

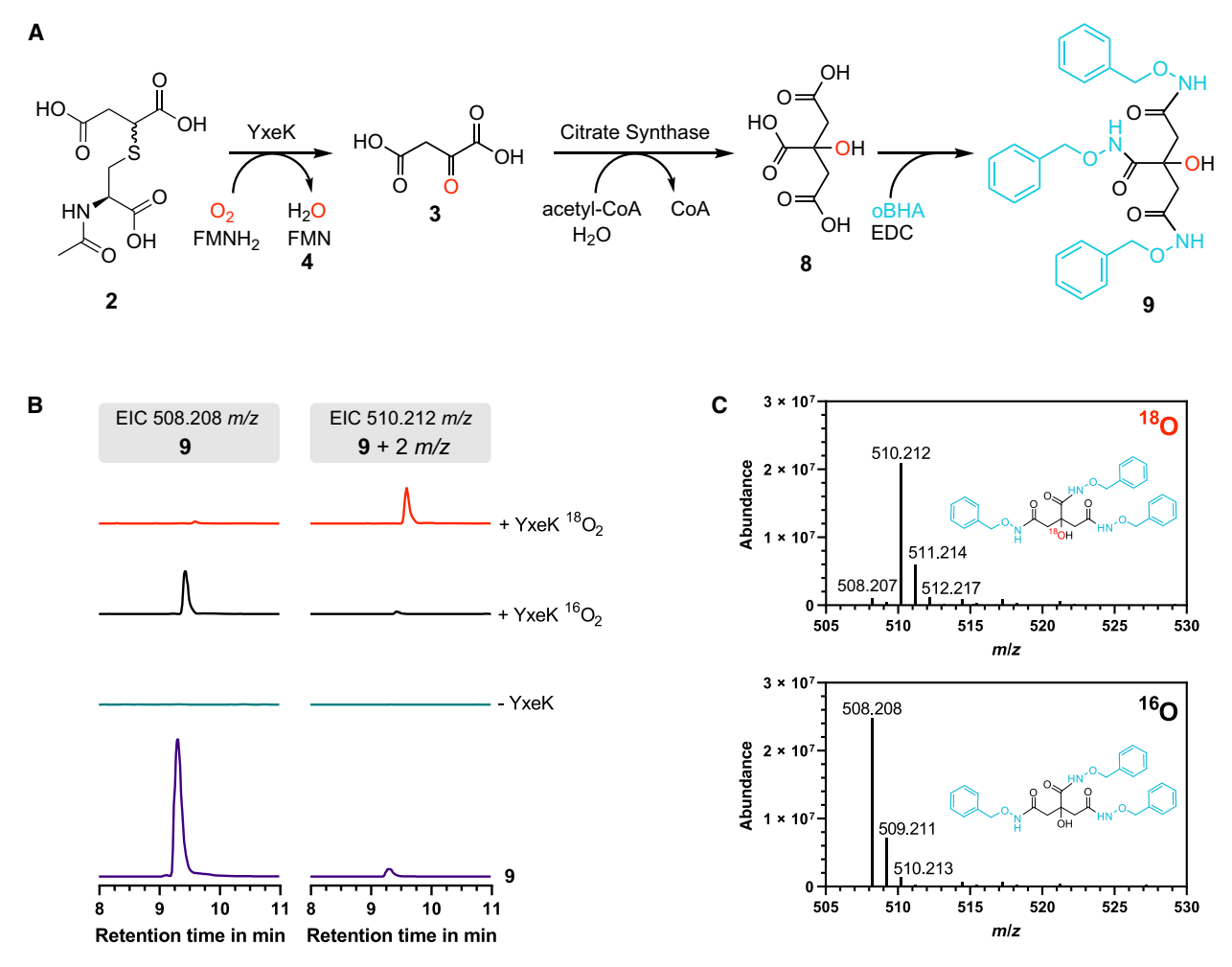


Fig. 3. UPLC-HRMS analysis (ESI, positive ion mode) of the YxeK-catalyzed reaction in presence of $^{18}O_2$. (A) Scheme of the YxeK reaction and **3** derivatization to **9** for MS analysis. (B) EICs of masses corresponding to unlabeled **9** (produced in presence of $^{16}O_2$: 508.208 m/z, left side) and ^{18}O -labeled **9** (produced in presence of $^{18}O_2$: 510.212 m/z, right side). Shown are EIC traces from enzyme assays containing $^{18}O_2$ (red) or $^{16}O_2$ (black), a control without YxeK (green), and a standard of **9** (purple). Traces use equal scaling and the total length of the Y-axis corresponds to an ion count of $^{5}\times 10^{7}$. (C) Mass spectra and isotope distribution of the derivatized YxeK product **9** at 9.5 min with incorporation of ^{18}O (top) or ^{16}O (bottom). Approximately 95% ^{18}O was incorporated into **9**. Two independent, biological replicates (n=2) were analyzed, and representative samples are shown.

undefined [12,28,40]. Loop movement is regulated by the *cis* (closed) and *trans* (open) conformation of a pivotal prolyl-peptide bond [28], possibly acting as a universal lid-gating mechanism that controls substrate binding and catalysis for this subgroup of FPMOs.

As crystallization attempts with YxeK proved unsuccessful, homology modeling using the SWISS-MODEL server [42] was conducted with the open and closed conformation of EmoA (PDB ID 5DQP, 34.5% aa identity, 97% coverage) as well as CmoJ/YtnJ (PDB ID 6ASL, 48.1% aa identity, 97% coverage) as templates in order to gain further insights into substrate binding, enzymatic O₂ activation, and catalysis.

The obtained model structure suggested an active site architecture similar to EmoA, SsuD, and the verified N5-oxygenating group C FPMOs (RutA, HcbA1, and DszA/BdsA) [12,24,27,43], including the mobile lid-like loop region with its prolyl-peptide bond hinge (Fig. 6 A). In particular, the proposed substrate-binding and O₂ reaction sites were also predicted to be located on the *si*- and *re*-side of FMN, respectively (Fig. 6B) [12]. Compared to RutA, the cavity on the *si*-side of YxeK's FMN appeared more open and thus well suited to accommodate the sizable 2 (Fig. 6B). Additionally, various potentially positively charged residues (R330, R74, H358, H359, and H19) were found in the

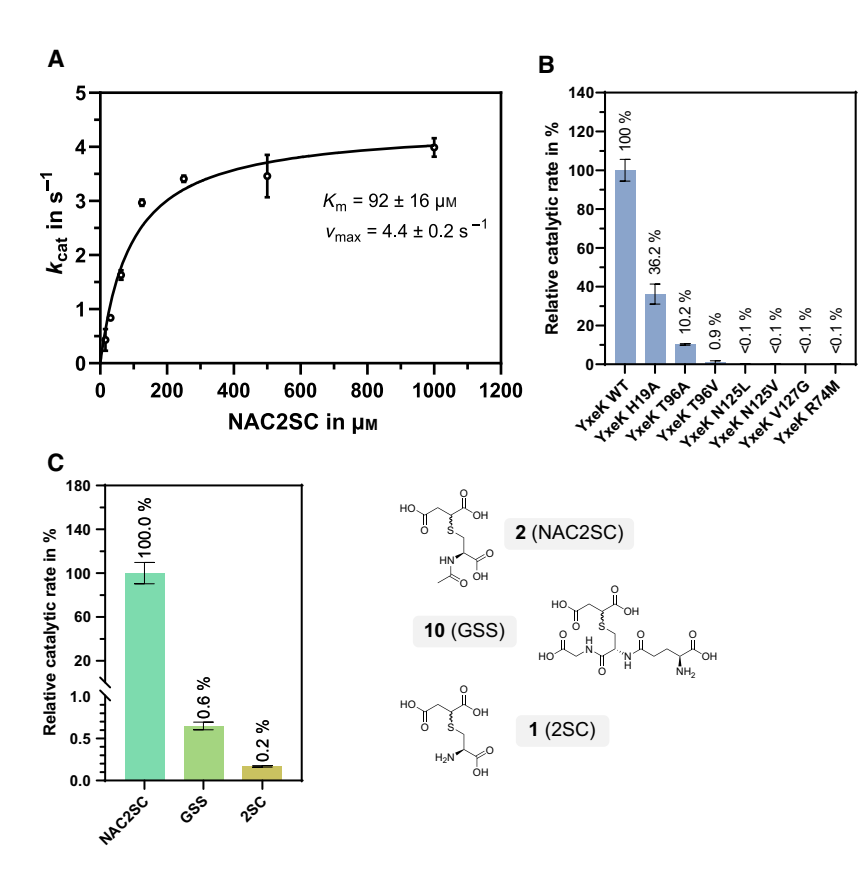


Fig. 4. (A) Determination of apparent kinetic parameters for reaction of YxeK with natural substrate **2** (NAC2SC) using Ellman's assay. (B) Comparison of catalytic rates between YxeK wt and variants. (C) Comparison of catalytic rates of YxeK wt with substrates **2** (NAC2SC), **10** (GSS), and **1** (2SC). For every condition in A–C, three independent biological replicates (n = 3) were analyzed. Mean values with standard error are displayed.

putative substrate-binding site that could interact with the carboxylate groups of 2 and/or promote catalysis. Although computational docking of 2 to YxeK using the DockThor server [44,45] was insufficient to predict the accurate substrate orientation, H19 is most likely in the direct vicinity of the site of oxidative attack. To investigate a possible role for this residue, a H19A YxeK variant was generated and investigated. The apparent k_{cat} of this variant was about 36% compared to the wild-type enzyme (Fig. 4B), suggesting only a minor role in catalysis. Furthermore, R74 of YxeK was replaced by a similarly sized nonpolar methionine residue (R74M variant), which resulted in almost complete abolishment of enzyme activity (Fig. 4B). The R74 side chain could thus be involved in substrate binding or catalysis but the exact role remains to be determined once a crystal structure becomes available.

Moreover, given the predicted high structural similarity of the proposed O_2 reaction pocket on the reside of FMN to RutA, a similar pathway for O_2 activation and FMN functionalization for YxeK appeared likely. To further investigate this, the putative O_2 -pocket-forming amino acid residues were mutated and the respective enzyme variants analyzed. As expected, replacement of T96A (for A/V), N125

(for L/V), and V127 (for G) completely abolished YxeK activity (Fig. 4B), in line with the proposed role of these residues for superoxide stabilization and promotion of regiospecific N5-oxygenation [1,12]. It is noteworthy that the crystal structure of the closely related alkanesulfonate monoooxygenase MsuD in complex with FMN and the substrate methanesulfonate was also recently reported, which also features the RutA-like O2 reactivity motif. The site of oxidative attack was shown to be in close proximity to the flavin-N5 position and thus consistent with a Fl_{N5OO} (H) species during catalysis [46]. DFT calculations with RutA corroborated the notion that an Fl_{N5OO} formed on the re-side can undergo a nitrogen inversion subsequent to its formation and thus bring the distal oxygen in contact with the substrate on the siside, whereas a hypothetical Fl_{C4aOO} would remain spatially separated from the substrate [1,12]. A similar scenario can thus be envisaged for YxeK comprising Fl_{N5OO} formation, nitrogen inversion, and final oxygen transfer. Taken together, these data suggest that YxeK may depend on N5-oxygen adducts (Fl_{N5OO} or the Fl_{N5O}) for catalysis rather than the classical Fl_{C4aOO(H)} species to facilitate the oxidative C-S bond cleavage of 2.

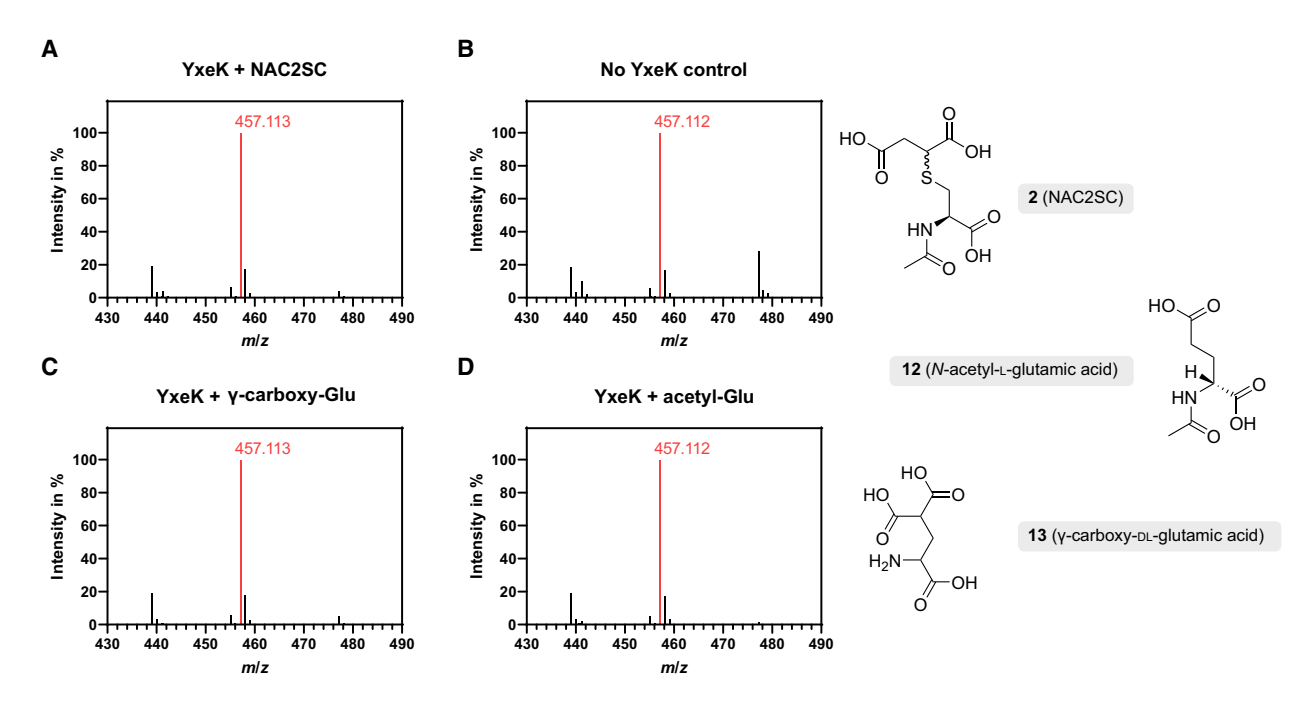


Fig. 5. Mass spectra from UPLC-HRMS analysis of flavin from YxeK standard assays with different substrates. Calculated [M + H]⁺ masses of FMN and FMN-N5-oxide are 457.112 m/z and 473.107 m/z respectively. (A) YxeK standard assay with natural substrate **2.** (B) Control assay without YxeK. (C) YxeK standard assay with compound **13** as substrate. (D) YxeK standard assay with compound **12** as substrate. The mass of FMN-N5-oxide was not detectable in any assay.

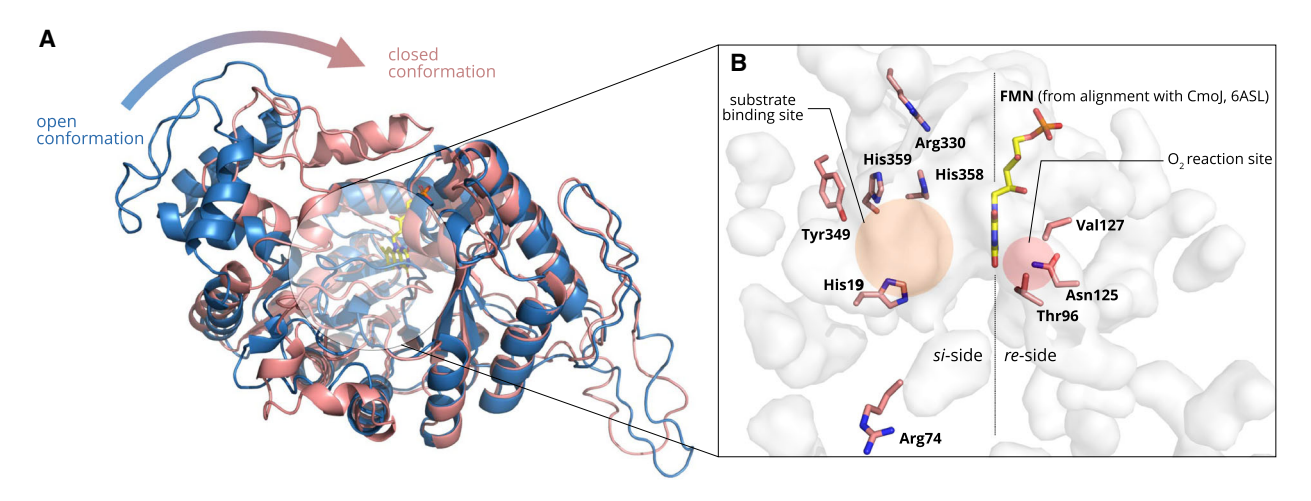


Fig. 6. (A) Homology model of YxeK produced with the SWISS-MODEL server using the open (blue) or closed (red) form of EmoA (PDB ID 5DQP) as a template. (B) View of the YxeK active site in the putative closed confirmation. FMN was placed in the model through alignment with the closely related cysteine salvage pathway monooxygenase CmoJ/YtnJ (PDB ID 6ASL). YxeK features two putative sites for substrate-binding (orange) and O₂ activation (red) on the *si-* and *re-*side of the FMN cofactor respectively.

Stopped-flow spectroscopic analysis of the reaction of YxeK-Fl $_{red}$ with O_2 and \emph{N} -acetyl- \emph{S} -(2-succino)-L-cysteine

To further investigate the reaction of YxeK with O_2 , samples containing FMN_{red} and YxeK were mixed

with O₂ alone or O₂ combined with **2** and then analyzed by stopped-flow spectroscopy (Fig. 7A–D). In the absence of **2**, the YxeK-Fl_{red} complex oxidized fairly slowly into YxeK-Fl_{ox} without observable intermediates and the traces at all wavelengths fitted to a

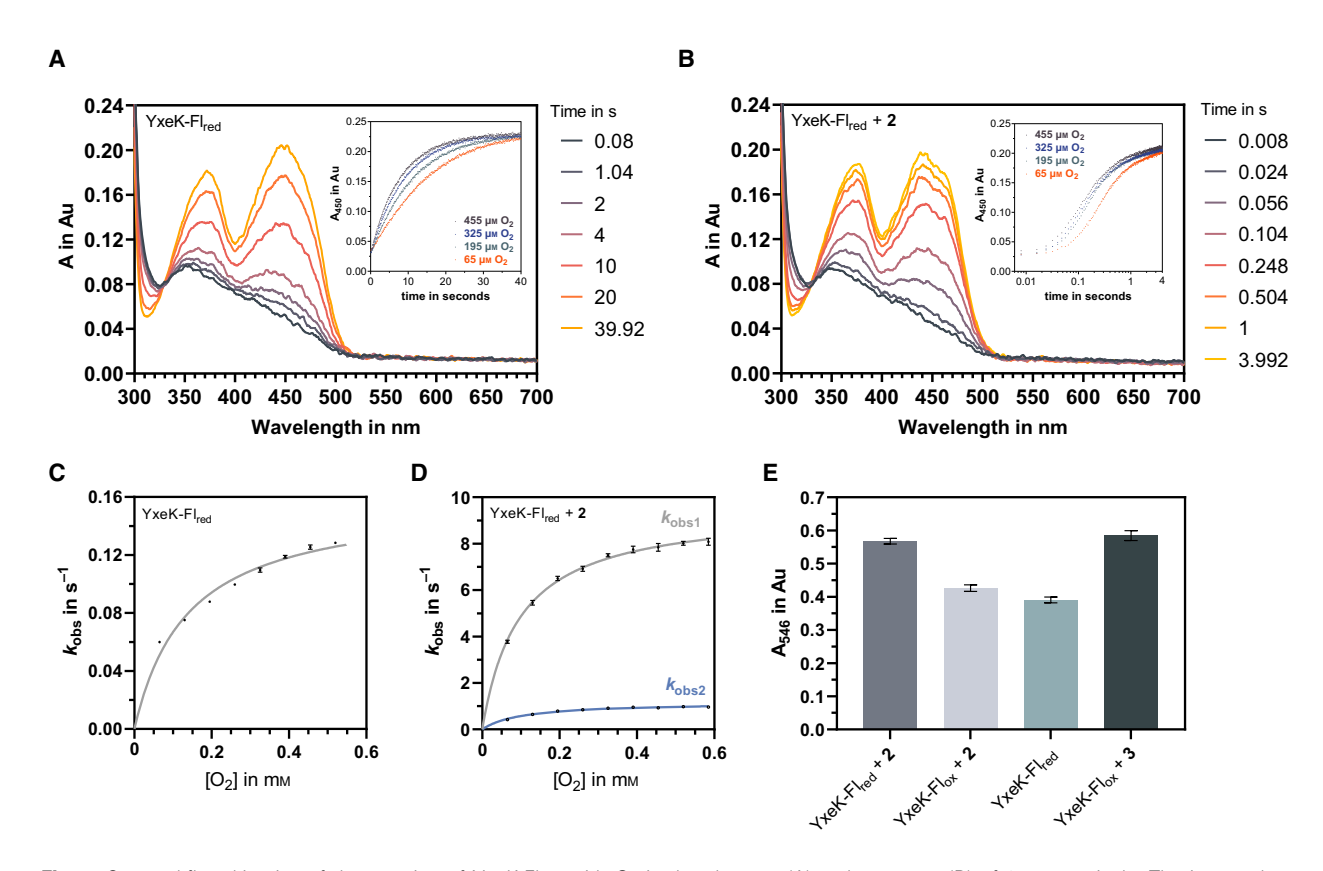


Fig. 7. Stopped-flow kinetics of the reaction of YxeK-Fl_{red} with O_2 in the absence (A) and presence (B) of **2**, respectively. The insets show the kinetic traces at 450 nm for each experiment under varying O_2 concentrations (the X-axis of the inset in panel B is displayed in a base 10 logarithmic scale). The kinetic trace in panel A fit to a single exponential whereas the kinetic trace in panel B fit best to a sum of two exponentials. Plots of k_{obs} against $[O_2]$ in absence and presence of **2** are shown in panels (C) and (D), respectively. The reaction in B formed **3** in a 1 : 1 ratio with the starting $[Fl_{red}]$ as determined by a DNPH colorimetric assay (E) (n = 3); error bars error bars represent the standard deviation).

single exponential. In contrast, when 2 was added, O2 oxidized YxeK-Fl_{red} significantly faster with the traces at all wavelengths fitting best to a double exponential. The reaction traces were the same when aerobic YxeK (in the absence or presence of 2) was mixed with FMN_{red}, indicating that premixing YxeK and FMN_{red} does not prevent the formation of a flavin-oxygen intermediate like it does in some flavin-dependent halogenases [47]. The first phase comprised ~80% of the total signal change at 450 nm and ended at ca. 0.5 s with an absorbance spectrum resembling Flox. The slower second phase appeared to involve further cofactor oxidation and possibly resulted from multiple YxeK populations. The spectra of the first time point for both tested conditions were virtually identical and indicative of fully reduced FMN, implying that no spectral intermediates were missed within the dead time of the instrument. The final absorbance spectrum, however, was different in the presence of 2; that is, the A450 peak was more featured with a blue-shifted

maximum of ~440 nm (versus 446 nm in the absence of 2), likely caused by binding of 2 or products 3 and 4 in the active site. This could be verified by addition of 2 to aerobic YxeK-Flox, which triggered similar spectral changes and thus implied that the native substrate expectedly binds in the direct vicinity of the FMN cofactor in YxeK (similar effects were observed for addition of 2 to YxeK-Fl_{N5O}, see below) (Fig. 8A,B), whereas incubation of YxeK-Flox with product 3 alone did not alter the flavin UV-Vis spectrum (Fig. 8C). The observed rate constants (kobs) in the absence and presence of 2 displayed an unusual hyperbolic dependence on the O2 concentration, reaching saturating values at high O₂ concentrations (Fig. 7A-D). This pattern was observed previously for the reaction of EncM-Fl_{red} with O₂ to form EncM-Fl_{N5O} [11] and suggests that O2 first binds to YxeK before reacting with Fl_{red} to form Fl_{ox} . The apparent K_d obtained from the fit of k_{obs} against O_2 concentration was $140 \pm 10 \,\mu M$ in the absence of 2 (Fig. 7C) and ~100 µm for both

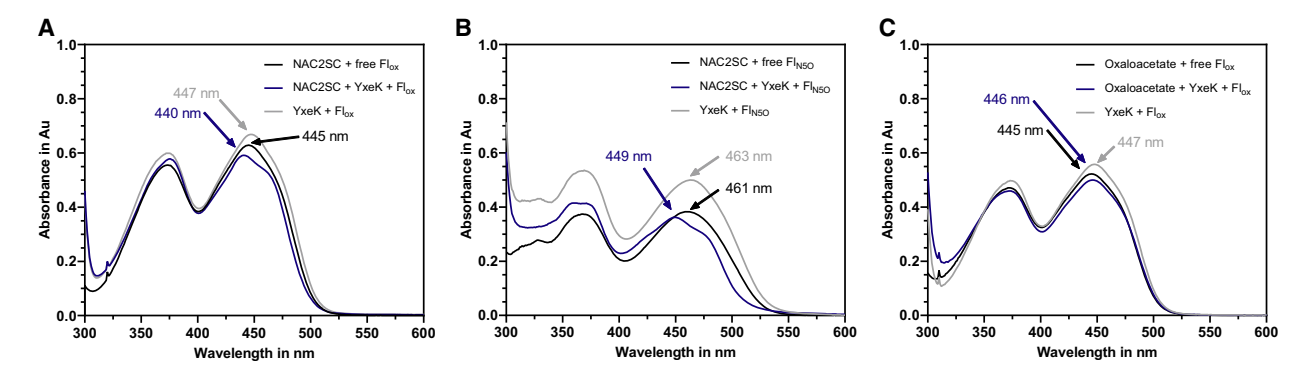


Fig. 8. (A–C) UV-Vis spectra of free flavin cofactors (Fl_{0x} or Fl_{N5O}) with substrate 2 (NAC2SC) or product 3 (oxaloacetate) (black lines), YxeK with flavin cofactors and 2/3 (blue lines) and YxeK with flavin cofactor without 2/3 (gray lines). Spectra of free flavin with 2/3 were identical when either directly mixed or when enzyme was added and subsequently heat-denatured. The blue-shift of the flavin absorption maximum to 449 and 440 nm (for Fl_{N5O} and Fl_{0x} respectively) indicates that substrate binding may induce conformational changes of YxeK.

phases in the presence of **2** (Fig. 7D), suggesting that **2** binding does not have a major effect on the affinity of YxeK for O_2 . However, the rate constant for Fl_{red} oxidation (k_{ox}) by O_2 was substantially greater when **2** was present (9.5 s⁻¹ and 1.2 s⁻¹ for the two phases in the presence of **2** vs 0.16 s⁻¹ in the absence of **2**), indicating that **2** accelerates Fl_{red} oxidation by O_2 . The reaction of YxeK- Fl_{red} with **2** in the stopped-flow spectrophotometer afforded **3** in a 1:1 ratio with the starting [Fl_{red}] as determined by a DNPH colorimetric assay (Fig. 7E).

As Fl_{red} oxidation is accelerated by the addition of 2, this points toward a strategy to couple O2 activation and FMN oxygenation to the presence of substrate and thereby minimize H₂O₂ formation and futile redox cycles. This could go along with conformational changes such as lid closure over the active site, conceivably as a requisite for efficient O2 reaction with FMN_{red}. A comparable substrate 'proofreading' mechanism prior to flavin oxygenation is for instance employed by group A FPMOs [1,4]. Notably, no spectroscopic evidence of putative intermediates such as transient Fl_{C4aOO(H)} or Fl_{N5OO(H)} species could be obtained during YxeK-Flred oxidation, similar to the previously reported reaction of Flred with O2 in RutA [12] and EncM [16]. In these cases, however, Fl_{N5O} species accumulated, suggesting that the envisaged Fl_{N5OO} (H) precursors may be too short-lived for detection, which could result from the high energy state and reactivity of this species [11,13]. EncM represents a structurally unrelated polyketide monooxygenase that employs an analogous O2 activation strategy to RutA [1,11,12]. In particular, EncM features a similar O₂ reaction site at the re-side of its covalently bound FAD cofactor, allowing the formation of a stable Fl_{N5O}

oxygenating species that is maintained in the resting state and most likely formed from a Fl_{N5OOH} precursor independent of the polyketide substrate. In contrast, RutA couples Flred oxidation and FlN5OO formation to the presence of uracil, thereby preventing wasteful use of NADH and decomposition of Fl_{N5OO} [1,12]. The observed accumulation of Fl_{N5O} during RutA catalysis therefore most likely results from Fl_{N5OO}-mediated cleavage of uracil via formal transfer of an [OH] that yields the product ureidoacrylate as well as Fl_{N5O} [12]. Remarkably, recently the first enzyme was reported that may combine Fl_{N5OO} and Fl_{N5O} catalysis, thus representing a novel flavoprotein dioxygenase prototype that structurally resembles acyl-CoA dehydrogenases [15]. In the case of YxeK, the final spectra suggested the exclusive formation of Flox (Fig. 7A), as further verified by UPLC-HRMS analysis (Fig. 5A-D). Assuming that YxeK initially reacts with O2 to an Fl_{N5OO} in the presence of substrate similar to RutA, this could indicate that the Fl_{N5O} is either not formed during catalysis or, alternatively, consumed during the cleavage reaction of 2 by serving as oxygen transferring species itself.

YxeK may employ an Fl_{N500} rather than Fl_{N50} for oxidative catalysis

To investigate the possible involvement of N5-oxygen adducts during YxeK catalysis, Fl_{N5O} (i.e., FMN_{N5O}) was chemoenzymatically synthesized for *in vitro* enzyme assays (Figs S3–S9). First, the binding of Fl_{N5O} to YxeK was examined by UV-Vis spectroscopy. In the presence of YxeK alone, the Fl_{N5O} spectrum remained stable, whereas the addition of 2 triggered clear spectroscopic changes, similar to the observations with Fl_{ox} described above, thus

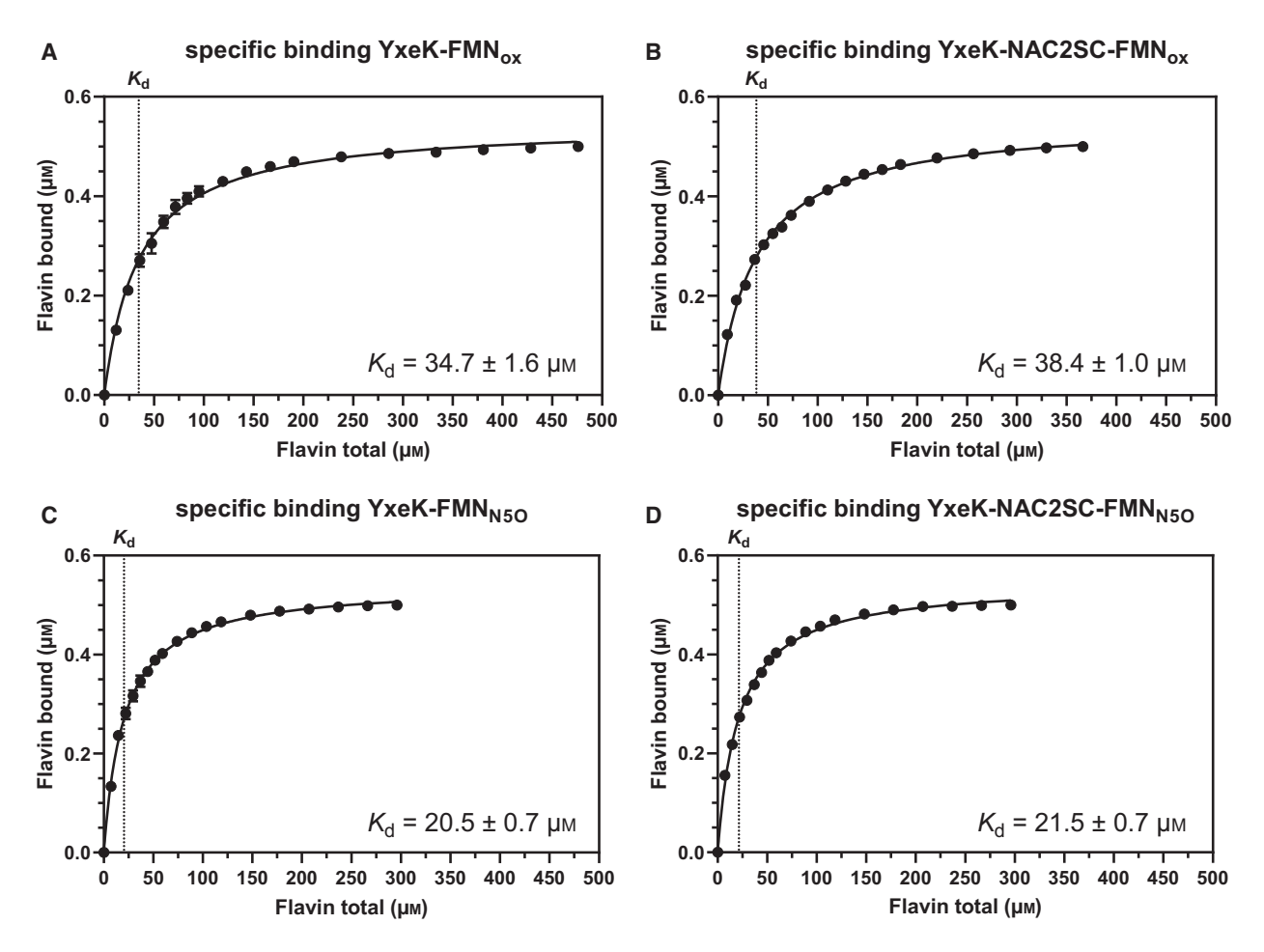


Fig. 9. Fluorimetric titration of YxeK in presence or absence of compound **2** with FMN_{ox} (A and B, respectively) or FMN_{N5O} (C and D, respectively). A 500 nm solution of YxeK was titrated with FMN_{ox} or FMN_{N5O} aliquots so that concentrations between 0 and 476 μm flavin were present. When compound **2** was included, a concentration of 1 mm was used. The sample was excited at a wavelength of 280 nm and the emission intensity at 344 nm was monitored. For every combination, three independent biological replicates (n = 3) were analyzed. Error bars represent the standard deviation. Change in fluorescence was converted to estimated concentration of bound FMN according to methods given in Gao *et al.* [49] and plotted against total FMN concentration. Calculated dissociation constants (K_d) with corresponding standard error are displayed and additionally marked with as a dotted line.

confirming that both **2** and Fl_{N5O} bind to YxeK (Fig. 8B). Next, binding affinities for both FMN redox states were determined through fluorescence spectroscopy (Fig. 9A–D). Aliquots of an FMN solution were added to an YxeK solution and the decrease in protein fluorescence emission intensity at 344 nm due to flavin binding was monitored. Moderate binding affinities with K_d values (mean \pm standard deviation) of 34.7 \pm 1.6 μ m (YxeK-Fl_{ox}), 38.4 \pm 1.0 μ m (YxeK-2-Fl_{ox}), 20.5 \pm 0.7 μ m (YxeK-Fl_{N5O}), and 21.5 \pm 0.7 μ m (YxeK-2-Fl_{N5O}) were observed, showing that the addition of substrate **2** had no significant effect on flavin affinity. The K_d for Fl_{ox} was slightly higher than for Fl_{N5O} but both in a similar range as determined for

SsuD (K_d of 10.2 \pm 0.4 μ M) that showed a clear preference for Fl_{red} (K_d of 0.32 \pm 0.15 μ M) [48].

A possible catalytic role for the Fl_{N5O} was subsequently investigated by *in vitro* enzyme assays. First it was tested, whether **2** can be directly converted into **3** and **4** by YxeK-Fl_{N5O} without prior flavin reduction (i.e., in the absence of Fre/NADH). However, no products were observed when the assay was derivatized with oBHA/EDC and analyzed via LC-HRMS (Fig. 10A), thus ruling out Fl_{N5O}-mediated oxidative substrate cleavage. Also, a two-step YxeK mechanism is conceivable that combines both Fl_{N5OO} and Fl_{N5O} catalysis and would involve Fl_{N5OO}-dependent (RutA-like) nonoxidative C–S bond cleavage to afford malate and

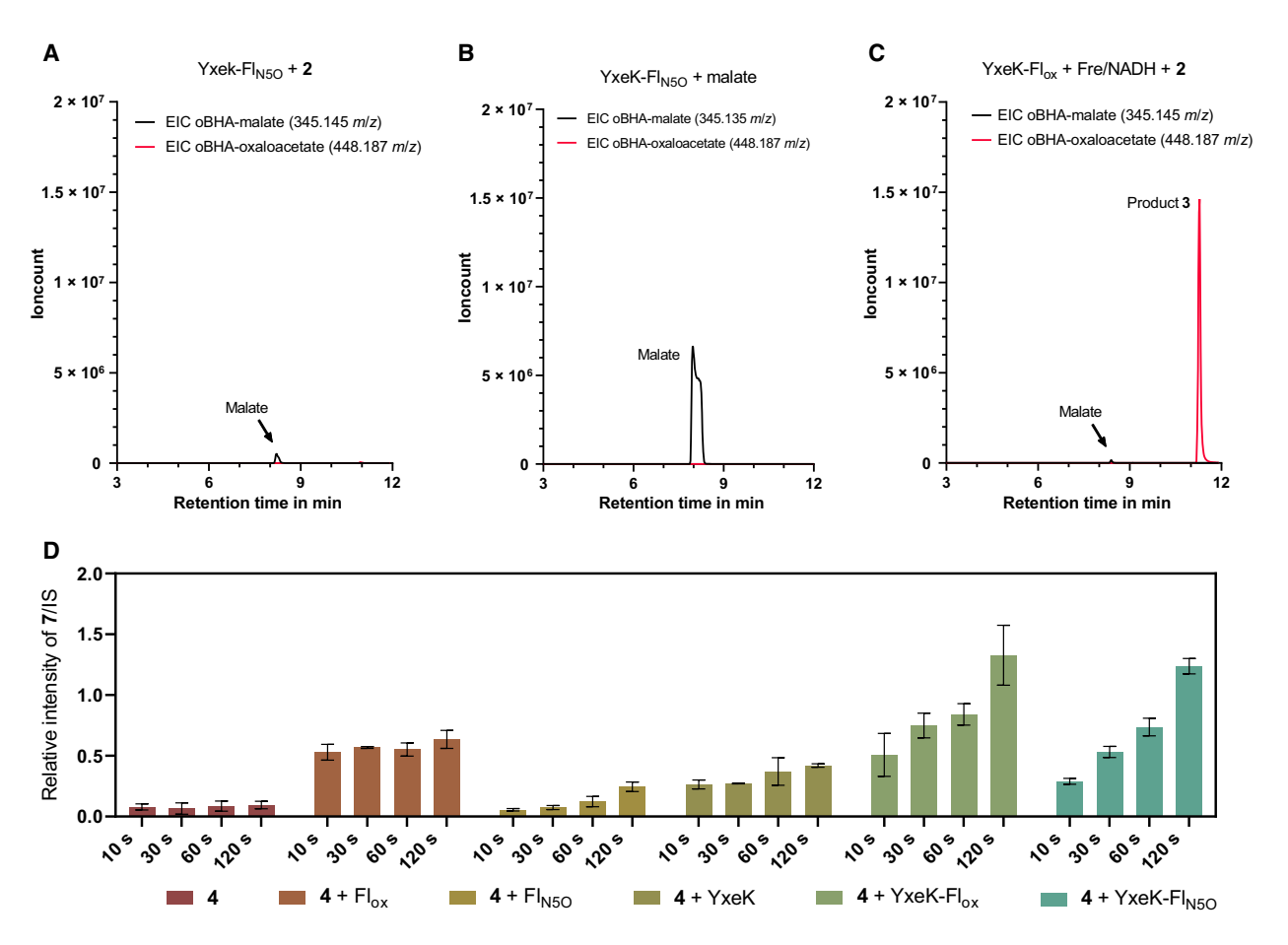


Fig. 10. (A–C) UPLC-HRMS analysis (ESI, positive ion mode) of assays analyzing the catalytic function of YxeK-Fl_{N5O}. EICs for the putative intermediate malate ([M + H]⁺ of oBHA-derivatized malate = 345.145 m/z, black lines) and product **3** (oxaloacetate, [M + H]⁺ of oBHA-derivatized **3** = 448.187 m/z, magenta lines) are shown. The natural substrate **2** (NAC2SC, A), as well as malate (B) were not converted to **3** by YxeK-Fl_{N5O}. A control assay showing a YxeK standard reaction with Fre-NADH and substrate **2** is showing the production of **3** (C). (D) LC/MRM-MS analysis (ESI, positive ion mode) showing relative intensities of **7** (DAC) in relation to the internal standard *O*-methyl-L-tyrosine for multiple time points. Oxidation and dimerization of compound **4** to **7** were tested through incubation of **4** with YxeK and/or either flavin cofactor (Fl_{Ox} or Fl_{N5O}). Formation of the disulfide **7** is accelerated in presence of enzyme and either flavin cofactor (n = 2; error bars represent the standard deviation).

4, followed by Fl_{N5O}-mediated alcohol oxidation of malate to 3. Accordingly, YxeK assays containing Fre-NADH and 2 were screened for the transient formation of malate and/or Fl_{N5O} by LC-HRMS. While Fl_{N5O} could not be observed under any conditions, low amounts of malate were detected. However, when incubated with YxeK-Fl_{N5O} (in presence or absence of 4), malate was not converted into 3 (Fig. 10B and Fig. S10A-C). As a control, oBHA-derivatized 3 was produced when YxeK-Flox was incubated with Fre/ NADH and 2 (Fig. 10C). Overall, these data are incongruous with a putative two-step oxidation mechanism. Further investigation by isotope-labeling experiments with H₂¹⁸O and LC-HRMS analysis revealed that malate arises from hydrolysis of 2 (Fig. 11A-C). Interestingly, this reaction only occurred in the presence of YxeK, suggesting that the enzyme binds and seemingly activates $\mathbf{2}$ for an attack by nucleophiles even in the absence of FMN. It is noteworthy that the incubation of YxeK-Fl_{N5O} with $\mathbf{4}$ (instead of $\mathbf{2}$) resulted in the rapid conversion of Fl_{N5O} into Fl_{ox}, suggesting a Fl_{N5O}-mediated oxidation of $\mathbf{4}$ (Fig. 12). Further experiments combined with LC/MRM-MS analysis revealed that the oxidative dimerization of $\mathbf{4}$ into $\mathbf{7}$ is indeed accelerated in presence of YxeK and either Fl_{ox} or Fl_{N5O} (Fig. 10D). While these observations may not be relevant for the YxeK catalytic mechanism, they provide insights into the chemical reactivity of the Fl_{N5O}.

A remaining possibility for N5-oxygen adduct-dependent YxeK catalysis is an oxidative cleavage mediated by the $Fl_{N5OO(H)}$. Accordingly, similar to RutA, YxeK-Fl_{N5OO} could act as an α -nucleophile and

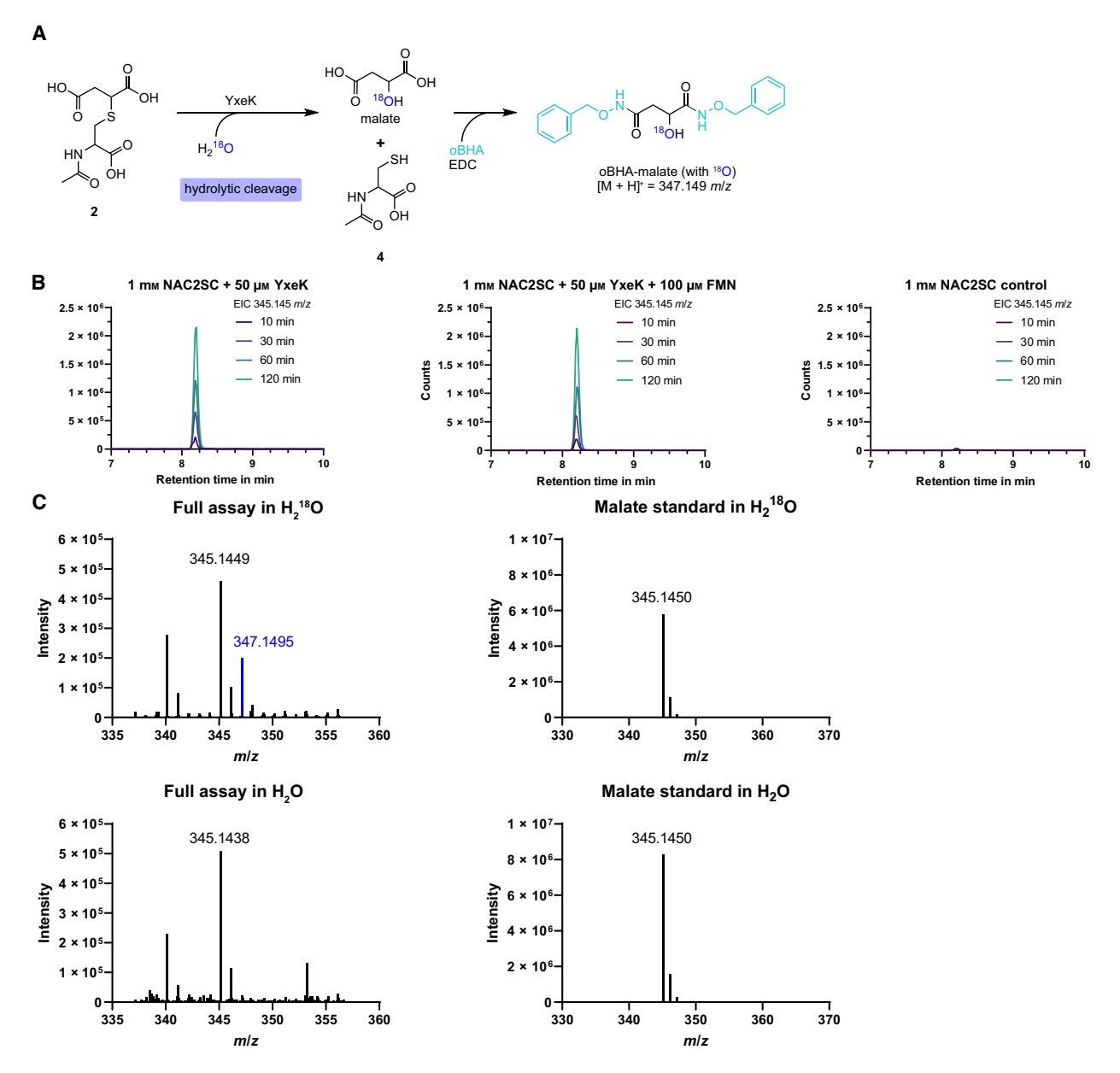


Fig. 11. UPLC-HRMS analysis (positive ion mode) of the YxeK-dependent production of malate through hydrolysis. (A) Scheme of proposed hydrolytic cleavage of **2** and subsequent oBHA/EDC derivatization of malate for UPLC-HRMS analysis. (B) Time course of malate production. Shown are EICs of 345.145 *m*/*z* corresponding to the [M + H]⁺ mass of oBHA/EDC-derivatized malate. Natural substrate **2** was incubated with YxeK (left panel), YxeK, and FMN (middle panel) or with enzyme buffer as a control (right panel). Samples were taken after 10, 30, 60, and 120 min and derivatized with oBHA/EDC. Malate is only produced in the presence of YxeK, regardless of cofactor presence. (C) Mass spectra of oBHA-derivatized malate from a standard assay with YxeK + Fre/NADH and compound **2** run in either 50% H₂¹⁸O (upper panels) and H₂O (lower panels). A malate standard (200 μM concentration) incubated simultaneously in the assay mixture without YxeK and Fre/NADH was used as a control for each condition. Incorporation of ¹⁸O from H₂¹⁸O into malate during hydrolytic cleavage by YxeK is indicated by the altered isotope pattern in which the oBHA-malate +2 *m*/*z* mass of 347.149 *m*/*z* is increased.

attack 2 to form a covalent intermediate under elimination of 4. This is supported by the observation that 2 is more susceptible to nucleophilic attack by water (when the proposed Fl_{N5OO} nucleophile is not present)

when bound by YxeK. Substrate activation could be achieved by a catalytic acid that protonates the sulfur of leaving group 4 and thus promotes C-S heteroatom bond cleavage. Then, a proton may be abstracted

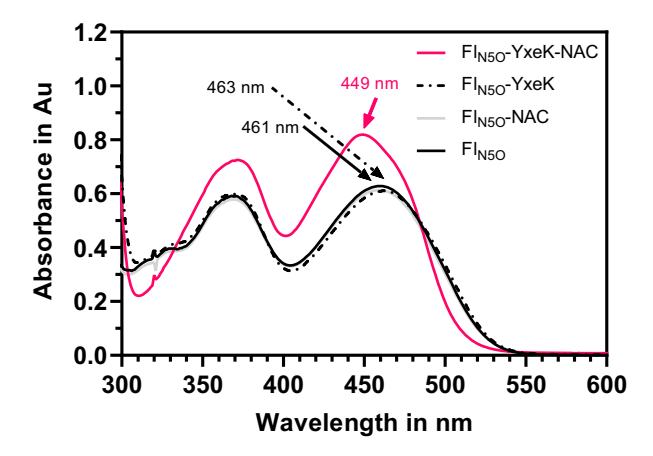


Fig. 12. UV-Vis spectra of enzyme-free FI_{N5O} (black line), FI_{N5O} incubated together with either compound **2** (NAC, gray line), enzyme YxeK (dotted black line), or both (magenta line). Conversion of FI_{N5O} to FI_{ox}, as indicated by the shift of the peak maximum from 463 to 449 nm, occurs rapidly when both YxeK and **2** are present.

presumably by the same amino acid residue from C2 of the covalently bound substrate remainder to trigger heterolytic peroxide cleavage via electron uptake by the FMN under concomitant release of 3 (Fig. 13). This last step would be distinct from RutA that mediates heterolytic peroxide cleavage with the substrate acting as the leaving group instead. In the YxeK homology model, side chains of multiple residues, including H19, are located close to the C-S bond and could act as proton donor. It is noteworthy that for SsuD, a critical R226 residue was identified that is likely similarly positioned and strictly requires protonation to enable catalysis [29].

As a variation of this mechanism, subsequent to covalent adduct formation via nucleophilic attack of 2 by the Fl_{N5OO}, YxeK could couple RutA-like heterolytic peroxide cleavage to hydride transfer from C2 of the substrate to the flavin, thereby affording 3. Lastly, although it is less likely, it is also conceivable that YxeK employs an electrophilic Fl_{N5OOH} that is attacked by 2, leading to a labile hemithioacetal intermediate via hydroxylation that spontaneously collapses to 4 and 3. YxeK could control this reaction by deprotonation of 2 and protonation of the aminoperoxide species to enhance nucleophilicity and electrophilicity, respectively (mechanisms not shown). In all these scenarios, the formed Fl_{N5OH} could eventually eliminate water to regenerate Flox (Fig. 13). However, mechanisms involving Fl_{C4aOO(H)} species cannot be ruled

out, as previously proposed, for example, for SsuD or EmoA prior to the discovery of N5-oxygenated flavins [19,28,29]. Summed up, our data clearly show that YxeK acts as an FMN-dependent monooxygenase catalyzing the oxidative cleavage of 2. However, the active site architecture and substrate-binding/activation mode of YxeK remain to be elucidated alongside the underlying oxygenation mechanism.

Conclusion

In this work, we verified the role of flavoprotein monooxygenase YxeK from B. subtilis in the salvaging and detoxification of N-acetyl-S-(2-succino)-L-cysteine that arises from the spontaneous Michael addition of the soft nucleophile cysteine to the electrophile fumarate. We furthermore show that YxeK exhibits a narrow substrate scope with a strong preference for its native substrate over the nonacetylated form or fumarate-glutathione adducts that are converted less efficiently. YxeK thus expands the enzymatic toolbox of monooxygenases that process sulfur-containing metabolites enabling bacteria to utilize them as sulfur sources. Bacillus subtilis was shown to possess multiple monooxygenases (CmoO, CmoI, and CmoJ), that partake in sulfur metabolism, of which CmoJ is most closely related to YxeK as a group C FPMO. However, substrate specificities seem to differ among these monooxygenases, as YxeK could not functionally replace any of the other enzymes in metabolic studies

Detailed investigation of YxeK suggested a RutAlike O2 reaction site, which points toward oxygenation and functionalization of FMN-N5 rather than C4a. The formed Fl_{N5OO} species could then facilitate the oxygen transfer to the substrate, a mechanism that may be shared by related group C FPMOs that catalyze similar oxidative carbon-heteroatom bond cleavage reactions such as SsuD, MsuD, or EmoA. Evidently, mechanisms relying on classical Fl_{C4aOO(H)} species cannot be ruled out based on our data and further studies will be required to solve this question, for example, by structural studies including O₂ pressurized X-ray crystallography as previously employed for RutA [12] and EncM [11] and further detailed computational and biochemical investigation. Taken together, the herein described YxeK-catalyzed oxygenative C-S bond cleavage of N-acetyl-S-(2-succino)-L-cysteine provides novel insights into bacterial sulfur metabolism and the exploitation and salvaging of pervasive metabolic dead-end products enabled by the mechanistically versatile flavoprotein monooxygenases.

Fig. 13. Mechanistic proposal for the YxeK-catalyzed oxidative cleavage of **2** involving a nucleophilic FI_{N5OO} species. Following the nucleophilic attack by the FI_{N5OO}, acid-base catalysis may enable heterolytic peroxide cleavage with the flavin as leaving group. FI_{N5OH} is formed at the end, which could eliminate water to restore FI_{ox}. Note that in the case of the previously reported nonoxidative carbonheteroatom bond cleavage reactions by related enzymes (e.g., RutA), the FI_{N5O} is formed as a stable by-product, which represents a superoxidized flavin species in contrast to the FI_{N5OH} shown here (same oxidation state as FI_{ox}). Other mechanisms involving FI_{N5OOH} or FI_{C4aOO(H)} species cannot be ruled out (see text). R = ribitylphosphate. B = Base.

Materials and methods

Chemicals and materials

Chemicals and reagents were purchased from Merck KgaA/ Sigma-Aldrich Chemie GmbH (Taufkirchen, Germany), Carl Roth (Karlsruhe, Germany), Fisher Scientific GmbH (Schwerte, Germany), and Biomol GmbH (Hamburg, Germany). Chemicals, enzymes, and materials for molecular cloning were purchased from Thermo Fisher Scientific/Life Technologies GmbH (Darmstad, Germany), New England BioLabs GmbH (Frankfurt am Main, Germany), and QIAGEN GmbH (Hilden, Germany). Oligonucleotides were obtained from Sigma-Aldrich. Materials for protein purification were obtained from GE Healthcare (Solingen, Germany), Bio-Rad Laboratories GmbH (Feldkirchen, Germany), Pall Corporation (New York, NY, USA), and Thermo Fisher Scientific. N-acetyl-2succinocysteine (NAC2SC), 2-succino(cysteine) (2SC), and Ssuccinylglutathione (GSS) were produced according to ref. [30] and purified by preparative HPLC in combination with a Eurospher II 100-5 C18, 250 x 20 mm column (KNAUER Wissenschaftliche Geräte GmbH, Berlin, Germany). Fractions containing desired product (detected by absorbance at 254 nm) were collected; successive runs were pooled, lyophilized, and stored at -20 °C. Stock solutions were prepared in distilled water. The identity of NAC2SC, 2SC, and GSS was confirmed by UPLC-HRMS. Additionally, MS² spectra of NAC2SC and 2SC were compared to published data in the MoNA database (entry MoNA001201 and MoNA001200, respectively).

Gene cloning, heterologous expression, and protein purification

The yxeK gene was amplified from genomic DNA of Bacillus subtilis strain 168 and subsequently cloned into

the pET28b vector (Novagen, Merck KgaA, Taufkirchen, Germany) using Fast Digest XhoI and BamHI (Thermo Fisher Scientific) as restriction enzymes for overexpression. Expression host E. coli BL21 (DE3) (Thermo Fisher Scientific) was transformed with the recombinant pET28byxeK plasmid. 10 mL of LB medium, inoculated with E. coli BL21 (DE3) containing pET28b-yxeK, was supplemented with 50 μg·mL⁻¹ kanamycin and grown at 37 °C overnight while shaking at 180 rpm. 500 mL of Terrific broth (TB medium) supplemented with 50 μg·mL⁻¹ kanamycin and 0.1% antifoam SE-15 was inoculated with 5 mL of the starter culture and grown until an OD_{600} of 0.5-0.6 was reached. Then, the culture was induced by adding IPTG to a final concentration of 250 µM, temperature was set to 18 °C, and the cells were grown shaking at 125 rpm for 16-20 h. Cells were harvested by centrifugation at 4000 g for 10 min at 4 °C. Cell pellets were resuspended in buffer A (50 mm HEPES pH 7.4, 150 mm NaCl) supplemented with 1 µM phenylmethylsulfonyl fluoride (PMSF) and lysed by sonication. Cell debris was removed by centrifugation at 18 000 g for 30-60 min at 4 °C. The supernatant was filtered through a 0.45-μM syringe filter prior to loading on a 5 mL HisTrap HP Ni²⁺nitrilotriacetate column (GE Healthcare) connected to a FPLC system (ÄKTA pure 25, GE Healthcare Life Science). Unbound protein was removed by washing with 4% buffer B (50 mm HEPES pH 7.4, 150 mm NaCl, 500 mm imidazole), and bound N-terminally His-tagged YxeK was then eluted by gradient elution from 4% to 100% buffer B over 6 column volumes. The protein was concentrated using a 10 kDa MW cutoff MACROSEP spin column (Pall Cooperation) and then either desalted with a 5 mL HiTrap desalting column (GE Healthcare) or further purified by size-exclusion chromatography utilizing a HiLoad 16/600 Superdex 200 pg column (GE Healthcare) equilibrated with buffer A and connected to a FPLC system. The identity and purity of the eluted protein were confirmed by SDS/PAGE. Purified protein aliquots were flash-frozen in liquid nitrogen prior to storage at -80 °C. Variants of YxeK were purified analogously using the above-described protocol. Gene cloning, heterologous expression, and protein purification of the *E. coli* flavin reductase (Fre) were performed following previously published protocols [12].

Site-directed mutagenesis

Mutations in pET28b-vxeK were introduced through PCR-based mutagenesis using oligonucleotides synthesized by Sigma-Aldrich (Table S1). First, amplification over seven cycles of pET28b-yxeK using separate reactions with forward and reverse oligonucleotides, respectively, was performed using the Q5 High-Fidelity DNA Polymerase (New England Biolabs) according to the manufacturer's protocols. Forward and reverse reactions were then combined and amplified for further 30 cycles. PCR products were digested with FastDigest DpnI (Thermo Fisher Scientific) to remove template DNA and E. coli TOP10 was transformed with the recombinant plasmid. Mutations were confirmed by sequencing (Eurofins Genomics Germany GmbH, Ebersberg, Germany). The yxeK H19A mutation was created through custom gene synthesis and cloned to a pET28b vector (BioCat GmbH, Heidelberg, Germany). Recombinant plasmids containing desired mutations were brought into the expression host E. coli BL21 (DE3) and the respective protein variants were produced and purified according to the procedures described in this work.

Sample derivatization with DNPH for HPLC and LC-MS analysis

A 5 mm solution of 2,4-dinitrophenylhydrazine (DNPH) in 1 m HCl was prepared. Assays with 100 μ L volume were stopped by addition of 25 μ L DNPH solution and incubated for 15 min at 30 °C. Assays were neutralized by addition of 25 μ L 1 m NaOH and proteins were separated afterward by centrifugation at 18 000 g for 10 min.

Sample derivatization with EDC and oBHA

Solutions of 0.5 M *O*-benzylhydroxylamine hydrochloride (oBHA) and 0.5 M 1-(3-dimethylaminopropyl)-3-ethylcarbodiimide hydrochloride (EDC) in pyridine buffer (8.6 mL pyridine, 5.4 mL HCl, and 86 mL distilled water) were prepared according to Tan *et al.* [51]. Assays were stopped by addition of 1 volume of methanol. Protein was precipitated by centrifugation at 18 000 g for 5 min. 50 μ L of the supernatant was mixed with 10 μ L of oBHA solution, 10 μ L of EDC solution, and 100 μ L ddH₂O and incubated

at 25 °C for 15–20 min under shaking at moderate speed. The aqueous phase was extracted twice with 200 μ L ethyl acetate and the organic phase was evaporated under reduced pressure afterward. Samples were resuspended in 100 μ L of a 30% acetonitrile/70% ddH₂O solution.

YxeK standard assay to determine reaction products

A solution of 50 mm HEPES pH 7.4, 1 mm substrate, 100 µm FMN, 1 µm His-Fre, and 1.5 mm NADH was prepared. Noncleavable substrates N-acetyl-L-glutamic acid (Sigma-Aldrich) and y-carboxyl-DL-glutamic acid (Sigma-Aldrich) were added in concentrations of up to 7 mm. After complete reduction of FMN at 30 °C without shaking, His-YxeK was added to a final concentration of 50 µm. The reaction was further incubated at 30 °C for 2 min while shaking vigorously. The reaction was stopped and derivatized with either DNPH or oBHA/EDC as described above. For analysis of flavin cofactor content or NAC/DAC formation, no derivatization was performed. Samples were then subjected to UPLC-HRMS analysis using an Acquity UPLC HSS T3 column. For analysis of different time points, a larger assay volume was chosen and samples were taken after 10, 30, 60, or 120 min of incubation. The reaction was stopped with an equal volume of methanol and derivatized with oBHA/EDC as described above.

Ellmann's assay to determine kinetic parameters of the YxeK/Fre-NADH reaction

A 10 mm stock solution of 5,5'-dithiobis-(2-nitrobenzoic acid) (DTNB or Ellman's reagent, Sigma-Aldrich) was prepared in reaction buffer (100 mm Tris/HCl, pH 8.0). Assays were prepared in reaction buffer and contained 100 µM DTNB, 20 µm FMN, 1 mm substrate, 1.5 mm His-Fre, 0.1 mg·mL⁻¹ catalase (from bovine liver powder, Sigma-Aldrich), and an appropriate amount of His-YxeK (75-375 nm YxeK for measurements with YxeK WT/variants or 3-60 µm YxeK for measurement with alternative substrates 2SC and GSS). For K_M determination, 75 nm His-YxeK was used and NAC2SC substrate concentration was varied (16, 31, 62, 125, 250, 500, and 1000 µm). Assays were transferred to a 10-mm QS quartz cuvette (Hellma Analytics) and absorbance at 412 nm was continuously monitored in a UV-1800PC photometer (Shimadzu Corp.). The reaction was allowed to equilibrate for 2 min before the reaction started by addition of NADH to a final concentration of 1 mm. For all assays, three independent biological replicates (n = 3) were prepared and measured. Apparent k_{cat} and K_M values were calculated based on the Lambert-Beer law using the extinction coefficient of produced 2-nitro-5thiobenzoic acid (TNB²⁻) of 13 600 M⁻¹·cm⁻¹ at 412 nm and pH 8.0 [52,53].

UV-Vis spectroscopy of YxeK-Fl_{ox} and YxeK-Fl_{N5O} to test influence of substrate binding

A solution containing 50 mm HEPES buffer (pH 7.5), 50 μM F_{lox} , or Fl_{N5O} with and without 500 μM NAC2SC was prepared. Spectra ranging from 300 to 600 nm with, without and with heat-denatured His-YxeK (50 μM end concentration) were recorded in a 10 mm QS quartz cuvette (Hellma Analytics) using a UV-1800PC photometer (Shimadzu Deutschland GmbH, Duisburg, Germany). Additionally, a control containing only $F_{lox}/$ Fl_{N5O} and/or NAC2SC was prepared and analyzed. Influence of NAC on the YxeK-Fl_N5O spectrum was tested using the above-described protocol with the exception of using 1 mm NAC in the sample solution instead of NAC2SC.

Fluorimetric determination of flavin binding constants

Flavin binding constants for His-YxeK and FMN_{ox}/ FMN_{N5O} in presence or absence of compound 2 were determined by spectrofluorometric titration as described in Gao & Ellis [49]. A 100 µL solution containing 500 nm His-YxeK and 50 mm HEPES pH 7.5 was prepared and transferred to a 96-well plate (black/clear bottom, Corning Inc.). If compound 2 was present, an end concentration of 1 mm was used. Protein concentration was calculated using a molar extinction coefficient of 45 380 M⁻¹·cm⁻¹ at 280 nm. Concentration of FMNox was determined using a molar extinction coefficient of 12 020 M⁻¹·cm⁻¹ at 450 nm, whereas FMN_{N5O} concentrations were approximated by using the molar extinction coefficient of EncM-FAD_{N5O} of 9600 M⁻¹·cm⁻¹ at 460 nm [16]. Spectra were recorded on a SpectraMax iD5 plate reader (Molecular Devices GmbH, München, Germany) with an excitation wavelength of 280 nm and emission monitoring at a wavelength of 344 nm. For all samples, three independent biological replicates (n = 3) were measured.

H₂¹⁸O and ¹⁸O-labeling assays with YxeK

An assay solution of 50 mm HEPES pH 7.4, 500 μm NAC-2SC, 75 μm His-YxeK, 150 μm acetyl-CoA, and 1 unit of citrate synthase (ammonium sulfate suspension, from porcine heart, Sigma-Aldrich) as well as a solution of 500 μm FMN and 10 mm EDTA was made anaerobic by incubation in an anaerobic chamber at 10 °C for 12 h. FMN was photoreduced by light irradiation for 5 min with a 900 lumen LED torch. Fl_{red} was added to the assay solution so that a final concentration of 75 μm was reached. Assays were incubated for a further 30 min before they were transferred to a Schott bottle with an airtight rubber seal and removed from the anaerobic chamber. The reaction was started by injection of >97% ¹⁸O₂ gas (Campro Scientific, Berlin, Germany) and

incubated for 2 hours at room temperature. A control reaction was conducted with atmospheric O_2 instead. One volume of methanol was added to one volume of reaction solution to quench the reaction. Sample derivatization with oBHA and EDC was performed as described above. Samples were analyzed by UPLC-HRMS. Assays with $H_2^{18}O$ were performed according to the protocol of standard YxeK assays with at least 50% (v/v) of $H_2^{18}O$ in the reaction mixture, derivatized with oBHA/EDC, and subjected to UPLC-HRMS analysis.

Assay to analyze dimerization rate of compound 4

An assay solution of 50 mm HEPES pH 7.4 and 100 μ m compound 4 was incubated with 50 μ m FMN_{ox} or 50 μ m FMN_{N5O} and/or 20 μ m YxeK for 10, 30, 60, and 120 s at 30 °C. The assays were quenched by adding 9 volumes of methanol containing 1 μ g·mL⁻¹ *O*-methyl-L-tyrosine as internal standard (IS) to 1 volume of assay solution. After centrifugation (20 000 g, 10 min, 4 °C), assays were subjected to LC/MRM-MS analysis (positive ion mode). For all samples, two independent biological replicates (n=2) were measured.

RP-UPLC and UPLC-HRMS

Samples were prepared as described and kept at 8 °C during analysis. 5-7 µL of the sample was used for each injection. A Waters ACQUITY I-class UPLC (Waters GmbH, Eschborn, Germany) equipped with an ACQUITY UPLC Photodiode Array (PDA) detector was used in conjunction with a Waters Synapt G2-Si quadrupole time-of-flight mass (Q-TOF) spectrometer equipped with an ESI-source. An ACQUITY UPLC HSS T3, 100 Å, 1.8 μ m, 2.1 × 100 mm column (Waters) was used. The flow rate was set to 0.2 mL·min⁻¹. Solvent A was water supplemented with 0.1% formic acid (FA) and solvent B was acetonitrile supplemented with 0.1% FA. The following gradient was used: 2% B from 0-1 min, 2-60% B from 1-11 min, 60% B from 11-13 min, 60-2% B from 13-13.5 min, 2% B from 13.5-16 min. The column temperature was kept at 30 °C. The mass spectrometer was operated in either positive (3500 V) or negative ion polarity (-1500 V). The source temperature was kept at 100 °C, desolvation gas temperature at 300 °C with a flow of 600 L·h⁻¹. The nebulizer pressure was 3.0 bar. Mass spectra were acquired from 50- $1200 \ m/z$ in centroid mode and corrected by leucine enkephalin.

LC/MRM-MS

N,N'-Diacetylcystine (DAC) levels were acquired by targeted LC-MS (Agilent Technologies, Waldbronn, Germany:

G4220A, G4226A, G1316A, G6460A) analysis. 1 µL was injected on a BEH-Amide column (Waters, 2.1 × 150 mm, 1.8 um). Samples were maintained at 4 °C. Column temperature was set to 50 °C; flow was 0.6 mL·min⁻¹ with water supplemented with 0.1% formic acid (A) and acetonitrile supplemented with 0.1% formic acid (B). The gradient was as follows: 90% B for 0.1 min, to 85% B within 0.1 min, to 75% B within 0.8 min, to 40% B within 1 min, to 50% B within 0.1 min, hold for 2.9 min, to 90% B within 0.2 min, hold for 4.8 min. The ion source was set to 300 °C gas temperature at 7 L·min⁻¹ gas flow, 350 °C sheath gas temperature with 11 L·min⁻¹ sheath gas flow, 50 psi nebulizer pressure, 4 kV capillary voltage, and 500 V nozzle voltage. DAC was measured in positive polarity at 4 V cell accelerator voltage and 108 V fragmentor voltage via multiple reaction monitoring (MRM): Precursor ion: 325.1 m/z, product ions: 162.1 m/z, 122.1 m/z, 116.1 m/z at collision energies of 10, 40, 40 eV, respectively. Data acquisition was performed by Agilent MassHunter data acquisition B.08.02 and analyzed with Agilent MassHunter Quantitative Analysis B.07.01 SP2. Intensities (quantifier ion: $162.1 \, m/z$) were normalized to O-methyl-L-tyrosine.

Stopped-flow spectroscopy

Stopped-flow experiments were performed at 4 °C in 50 mm HEPES-KOH pH 7.5 using a TgK Scientific SF-61DX2 KinetAsyst stopped-flow instrument (TgK Scientific Limited, Bradford-on-Avon, UK). A solution containing 40 µm FMN and 60 µm YxeK was placed in a glass tonometer and made anaerobic by repeated cycling with vacuum and anaerobic argon [54]. The FMNox was reduced to FMN_{red} by titrating with a dithionite solution, and the progress of FMN reduction was monitored by UV/VIS using a Shimadzu UV-1900 spectrophotometer. The tonometer containing FMN_{red}/YxeK was loaded onto the stopped-flow instrument and was then mixed with buffer bubbled with various O₂/N₂ ratios (made using a Maxtec MaxBlend 2 gas mixer) in the absence or presence of 400 µm 2. The dissolved O2 concentration in the buffer solution was calculated using Henry's law constant for O_2 of 770 atm·M⁻¹. The subsequent reaction was monitored using the instrument's multi-wavelength charge-coupled device detector (1.6-ms data interval time). Kinetic traces at 450 nm were fit to either a single exponential or a sum of two exponentials using Kaleida-Graph to determine observed rate constants. Plots of kobs against the O₂ concentration were fit to the following equation:

$$k_{\text{obs}} = \frac{k_{\text{ox}}[O_2]}{K_d + [O_2]}.$$

DNPH colorimetric assay to detect production of 3 (oxaloacetate)

A 2 mm solution of DNPH in 1 m HCl was prepared. 100 μ L of reoxidized assay solution from stopped-flow spectroscopy experiments containing 40 μ m FMN_{red}, 60 μ m YxeK, and 200 μ m compound 2 (NAC2SC) was mixed with an equal volume of DNPH solution and incubated for 20 min at room temperature. Afterward, 67 μ L of a 6 m NaOH solution was added and the solution was incubated for 5 min before measuring the absorbance at 546 nm. As negative controls, an assay with FMN_{red} but without substrate 2 was derivatized and measured as described above. An assay containing 40 μ m FMN_{ox} and 60 μ m YxeK was spiked with 40 μ m compound 3 (oxaloacetate) and used as a positive control.

Attempted crystallization conditions and homology model

Crystallization attempts were performed with SEC purified His-YxeK in low-salt buffer (20mm HEPES, 10 mm NaCl, pH 7.4) using the sitting-drop vapor diffusion method at either room temperature or 4 °C. Drop ratio was set to 1:1 (protein to reservoir solution). Additionally, the presence of FMN in the protein solution (1 mm end concentration) was tested. The following commercially available screens were used: Crystal Screen HT (Hampton Research), Index Screen HT (Hampton Research), PEG/Ion HT (Hampton Research), SaltRx (Hampton Research), JBScreen PACT++ (Jena Bioscience), JBScreen JCSG++ (Jena Bioscience), JBScreen Pentaerythritol (Jena Bioscience), as well as Morpheus I, II, and III (Molecular Dimensions).

A homology model of YxeK was created using the SWISS-MODEL server [42] with the User Template option. The amino acid sequence of YxeK was obtained from Uni-ProtKB (database ID P54950). User templates comprised the open or closed form monomer of EDTA monooxygenase (EmoA) from *Chelativorans* sp. BNC1 taken from the crystal structure (PDB ID 5DQP), or the cysteine salvage pathway monooxygenase CmoJ with bound FMN (PDB ID 6ASL). 3D structure alignments were performed and visualized in PYMOL 2.2 (Schrödinger, LLC.). Attempted docking studies with compound 2 were performed using the closed form homology model of YxeK with an aligned FMN cofactor from CmoJ using the DockThor webserver [44,45].

Synthesis of FMN_{N5O} (19)

 FMN_{N5O} (19) was produced by a modified synthesis based on published procedures [25,55]

15: A solution of 3,4-dimethylaniline (14, 3.0154 g, 24.884 mmol), D-ribose (11.1536 g, 74.2929 mmol, 3.0 eq.), and NaCNBH₃ (4.7211 g, 75.129 mmol, 3.0 eq.) in MeOH (150 mL) was stirred for 114 h at rt. The solvent was removed under reduced pressure, and residual NaCNBH₃ was quenched by adding aqueous HCl solution (1 m, 100 mL). The resulting solution was neutralized using aqueous NaOH solution (1 m) and extracted with EtOAc (6 × 90 mL). The combined organic layers were dried over MgSO₄ and filtered, and the solvent was removed under reduced pressure. Recrystallization from MeOH provided compound 15 as a colorless solid (3.3669 g, 13.187 mmol, 53%).

¹H-NMR (600 MHz, CD₃OD): δ = 6.88 (d, ${}^{3}J_{5,6} = 8.1$ Hz, 1H, 5-H), 6.55 (d, ${}^{4}J_{2,6} = 2.2$ Hz, 1H, 2-H), 6.47 (dd, ${}^{3}J_{6,5} = 8.1$ Hz, ${}^{4}J_{6,2} = 2.2$ Hz, 1H, 6-H), 3.91 (ddd, ${}^{3}J_{2',1'} = 7.9$ Hz, ${}^{3}J_{2',3'} = 6.4$ Hz, ${}^{3}J_{2',1'} = 3.5$ Hz, 1H, 2'-H), 3.78 (dd, ${}^{2}J_{5',5'} = 11.2$ Hz, ${}^{3}J_{5',4'} = 3.5$ Hz, 1H, 5'-HH), 3.74 (ddd, ${}^{3}J_{4',3'} = 6.4$ Hz, ${}^{3}J_{4',5'} = 6.2$ Hz, ${}^{3}J_{4',5'} = 3.5$ Hz, 1H, 4'-H), 3.67-3.59 (2H, overlapping signals: dd, ${}^{2}J_{5',5'} = 11.2$ Hz, ${}^{3}J_{5',4'} = 6.2$ Hz, 5'-HH; dd, ${}^{3}J_{3',2'} = {}^{3}J_{3',4'} = 6.4$ Hz, 3'-H), 3.43 (dd, ${}^{2}J_{1',1'} = 12.8$ Hz, ${}^{3}J_{1',2'} = 3.5$ Hz, 1H, 1'-HH), 3.09 (dd, ${}^{2}J_{1',1'} = 12.8$ Hz, ${}^{3}J_{1',2'} = 7.9$ Hz, 1H, 1'-HH), 2.17 (s, 3H, Ar-CH₃), 2.12 (s, 3H, Ar-CH₃) ppm.

¹³C-NMR (151 MHz, CD₃OD): δ = 148.1 (Ar-C), 137.9 (Ar-C), 131.1 (C-5), 126.7 (Ar-C), 116.7 (C-2), 112.5 (C-6), 74.9 (C-3'), 74.4 (C-4'), 72.2 (C-2'), 64.6 (C-5'), 48.1 (C-1'), 20.1 (CH₃), 18.8 (CH₃) ppm.

16: A mixture of 15 (251.0 mg, 0.9831 mmol), 6-chlorouracil (172.5 mg, 1.177 mmol, 1.2 eq.), and dimethylformamide (78 μ L, 74 mg, 1.0 mmol, 1.0 eq.) was heated for 10 min at 155 °C under vigorous stirring. The crude product was dissolved in pyridine (6.0 mL), acetic anhydride (1.0 mL) was added dropwise, and the resulting solution was stirred overnight at rt. The solvent was removed under reduced pressure and the residue was dissolved in CH₂Cl₂ (60 mL). The solution was washed with H₂O (4 × 40 mL) and saturated NaCl solution (2 × 40 mL). The organic layer was dried over MgSO₄, filtered and the solvent was removed under reduced pressure. Flash chromatography on silica gel (CH₂Cl₂:MeOH = 95:5) provided compound 16 as a pale yellow solid (30.6 mg, 0.0574 mmol, 6%)

¹H-NMR (600 MHz, CDCl₃): δ = 8.69 (br. s, 1H, uracil-NH), 7.34 (br. s, 1H, uracil-NH), 7.23 (d, ${}^{3}J_{5,6} = 7.9$ Hz, 1H, 5-H), 6.95 (d, ${}^{4}J_{2,6} = 2.1$ Hz, 1H, 2-H), 6.93 (dd, ${}^{3}J_{6,5} = 7.9$ Hz, ${}^{4}J_{6,2} = 2.1$ Hz, 1H, 6-H), 5.35 (ddd, ${}^{3}J_{2',1'} = 10.0$ Hz, ${}^{3}J_{2',3'} = 3.6$ Hz, ${}^{3}J_{2',1'} = 2.4$ Hz, 1H, 2'-H), 5.25 (dd, ${}^{3}J_{3',4'} = 6.3$ Hz, ${}^{3}J_{3',2'} = 3.6$ Hz, 1H, 3'-H), 5.11 (ddd, ${}^{3}J_{4',3'} = 6.3$ Hz, ${}^{3}J_{4',5'} = 6.0$ Hz, ${}^{3}J_{4',5'} = 3.0$ Hz, 1H, 4'-H), 4.97 (s, 1H, uracil-CH), 4.27 (dd, ${}^{2}J_{5',5'} = 12.5$ Hz, ${}^{3}J_{5',4'} = 3.0$ Hz, 1H, 5'-HH), 4.05 (dd, ${}^{2}J_{5',5'} = 12.5$ Hz, ${}^{3}J_{5',4'} = 6.0$ Hz, 1H, 5'-HH), 4.00 (dd, ${}^{2}J_{1',1'} = 15.6$ Hz, ${}^{3}J_{1',2'} = 10.0$ Hz, 1H, 1'-HH), 3.73 (dd, ${}^{2}J_{1',1'} = 15.6$ Hz, ${}^{3}J_{1',2'} = 2.4$ Hz, 1H, 1'-HH), 2.29, 2.28 (2s, 6H, 2 × Ar-CH₃), 2.11 (s, 3H, Ac-CH₃), 2.03, 2.02 (2s, 6H, 2 × Ac-CH₃), 1.89 (s, 3H, Ac-CH₃) ppm.

¹³C-NMR (151 MHz, CDCl₃): δ = 170.7, 170.2, 169.8, 169.6 (4 × Ac-CO), 164.5, 153.5, 150.1 (3 × uracil-C), 140.1, 138.8, 136.6 (3 × Ar-C), 132.1 (C-5), 129.2 (C-2), 125.5 (C-6), 76.8 (uracil-CH), 70.2 (C-3'), 69.5 (C-2'), 69.4 (C-4'), 61.9 (C-5'), 52.0 (C-1'), 21.1, 20.9, 20.8, 20.6 (4 × Ac-CH₃), 20.0, 19.6 (2 × Ar-CH₃) ppm.

17: 16 (31.2 mg, 0.0585 mmol) was dissolved in acetic acid (1.5 mL) and NaNO₂ (20.4 mg, 0.296 mmol, 5.1 eq.) was added in the dark. The mixture was stirred for 3 h at rt. H₂O (3.0 mL) was added, and the solution was stirred for another 3 h at rt. The solvents were removed under reduced pressure and 17 was obtained as an orange solid (30.9 mg, 0.0551 mmol, 94%) after purification via flash chromatography on silica gel (CH₂Cl₂:MeOH = 95:5).

¹H-NMR (600 MHz, CD₃OD): δ = 8.21 (s, 1H), 7.84 (s, 1H), 5.73-5.60 (m, 1H), 5.58-5.49 (m, 1H), 5.47-5.40 (m, 1H), 5.20-4.90 (m, hidden under H₂O signal), 4.50 (d, J = 12.3 Hz, 1H), 4.25 (dd, J = 12.3 Hz, J = 6.2 Hz, 1H), 2.57 (s, 3H), 2.46 (s, 3H), 2.21, 2.20 (2s, 6H), 2.03 (s, 3H), 1.75 (br. s, 3H) ppm.

HRMS (ESI): calculated for $C_{25}H_{28}N_4NaO_{11}$ [M + Na]⁺ 583.1647, found 583.1649.

18: NH₃ in MeOH (7 m, 60 mL) was added to **17** (138.5 mg, 0.2471 mmol) in the dark and the solution was stirred overnight at rt. The solvent was removed under reduced pressure and the crude product was purified via HPLC (MeCN/H₂O, 10:90 to 35:65 over 22 min, 10 mL·min⁻¹, retention time 8.5 min) providing **18** as an orange solid (79.2 mg, 0.202 mmol, 82%).

¹H-NMR (600 MHz, DMSO-d₆): δ = 11.08 (br. s, 1H), 8.07 (s, 1H), 7.92 (s, 1H), 5.12-5.06 (m, 1H), 4.98-4.78 (m, 3H), 4.65-4.53 (m, 1H), 4.53-4.45 (m, 1H), 4.27-4.18 (m, 1H), 3.67-3.60 (m, 3H), 3.49-3.43 (m, 1H), 2.43 (s, 3H), 2.38 (s, 3H) ppm.

HRMS (ESI): calculated for $C_{17}H_{20}N_4NaO_7$ [M + Na]⁺ 415.1224, found 415.1224.

UV/Vis: $\lambda_{\text{max}} = 220, 272, 370, 460 \text{ nm}.$

19: The final product was obtained by enzymatic phosphorylation of 18 [56].

Acknowledgements

This work was supported by the Deutsche Forschungsgemeinschaft (DFG) by grant nos. TE 931/3-1, TE 931/4-1, and 235777276/GRK1976 (awarded to RT). The authors thank Dr. Boris Illarionov (University of Hamburg) for performing the phosphorylation of Fl_{NSO} . ES thanks the Hans-Fischer Gesellschaft for generous support.

Conflict of interest

The authors declare no conflict of interest.

Author contributions

AM planned and performed gene cloning, heterologous expression, and protein purification of wild-type enzyme as well as enzyme variants, conducted all enzyme assays, and created homology models. JS and ES conducted the chemical synthesis of the FMN_{NSO}. SL and BK planned and performed sample derivatization and mass spectrometry experiments. HE analyzed data, FS planned and conducted stopped-flow spectroscopy and wrote the respective section, and RT planned and analyzed the experiments and wrote the manuscript with contributions from AM and FS.

References

- 1 Toplak M, Matthews A & Teufel R (2021) The devil is in the details: the chemical basis and mechanistic versatility of flavoprotein monooxygenases. *Arch Biochem Biophys* **698**, 108732.
- 2 Teufel R, Agarwal V & Moore BS (2016) Unusual flavoenzyme catalysis in marine bacteria. *Curr Op Chem Biol* 31, 31–39.
- 3 Teufel R (2017) Flavin-catalyzed redox tailoring reactions in natural product biosynthesis. *Arch Biochem Biophys* **632**, 20–27.
- 4 Palfey BA & McDonald CA (2010) Control of catalysis in flavin-dependent monooxygenases. *Arch Biochem Biophys* **493**, 26–36.
- 5 Huijbers MME, Montersino S, Westphal AH, Tischler D & van Berkel WJH (2014) Flavin dependent monooxygenases. Arch Biochem Biophys 544, 2–17.
- 6 Romero E, Gómez Castellanos JR, Gadda G, Fraaije MW & Mattevi A (2018) Same substrate, many reactions: oxygen activation in flavoenzymes. *Chem Rev* 118, 1742–1769.
- 7 Walsh CT & Wencewicz TA (2013) Flavoenzymes: versatile catalysts in biosynthetic pathways. *Nat Prod Rep* **30**, 175–200.
- 8 Paul CE, Eggerichs D, Westphal AH, Tischler D & van Berkel WJH (2021) Flavoprotein monooxygenases: versatile biocatalysts. *Biotechnol Adv* **51**, 107712.
- 9 Chaiyen P, Fraaije MW & Mattevi A (2012) The enigmatic reaction of flavins with oxygen. *Trends Biochem Sci* **37**, 373–380.
- 10 Mattevi A (2006) To be or not to be an oxidase: challenging the oxygen reactivity of flavoenzymes. *Trends Biochem Sci* 31, 276–283.
- 11 Saleem-Batcha R, Stull F, Sanders JN, Moore BS, Palfey BA, Houk KN & Teufel R (2018) Enzymatic control of dioxygen binding and functionalization of the flavin cofactor. *Proc Natl Acad Sci USA* 115, 4909–4914.
- 12 Matthews A, Saleem-Batcha R, Sanders JN, Stull F, Houk KN & Teufel R (2020) Aminoperoxide adducts

- expand the catalytic repertoire of flavin monooxygenases. *Nat Chem Biol* **16**, 556–563.
- 13 Saleem-Batcha R & Teufel R (2018) Insights into the enzymatic formation, chemical features, and biological role of the flavin-N5-oxide. *Curr Opin Chem Biol* **47**, 47–53.
- 14 Massey V (1994) Activation of molecular oxygen by flavins and flavoproteins. *J Biol Chem* 269, 22459– 22462.
- 15 Duan Y, Toplak M, Hou A, Brock NL, Dickschat JS & Teufel R (2021) A flavoprotein dioxygenase steers bacterial tropone biosynthesis via coenzyme A-ester oxygenolysis and ring epoxidation. *J Am Chem Soc* 143, 10413–10421.
- 16 Teufel R, Miyanaga A, Michaudel Q, Stull F, Louie G, Noel JP, Baran PS, Palfey B & Moore BS (2013) Flavin-mediated dual oxidation controls an enzymatic Favorskii-type rearrangement. *Nature* 503, 552–556.
- 17 Teufel R, Stull F, Meehan MJ, Michaudel Q, Dorrestein PC, Palfey B & Moore BS (2015) Biochemical establishment and characterization of EncM's flavin-N5-oxide cofactor. *J Am Chem Soc* 137, 8078–8085.
- 18 Adak S & Begley TP (2017) RutA-catalyzed oxidative cleavage of the uracil amide involves formation of a flavin-N5-oxide. *Biochemistry* 56, 3708–3709.
- 19 Ellis HR (2010) The FMN-dependent two-component monooxygenase systems. Arch Biochem Biophys 497, 1– 12
- 20 Brodl E, Winkler A & Macheroux P (2018) Molecular mechanisms of bacterial bioluminescence. *Comput Struct Biotechnol J* 16, 551–564.
- 21 Loh KD, Gyaneshwar P, Markenscoff Papadimitriou E, Fong R, Kim K-S, Parales R, Zhou Z, Inwood W & Kustu S (2006) A previously undescribed pathway for pyrimidine catabolism. *Proc Natl Acad Sci USA* 103, 5114–5119.
- 22 Takagi K, Iwasaki A, Kamei I, Satsuma K, Yoshioka Y & Harada N (2009) Aerobic mineralization of hexachlorobenzene by newly isolated pentachloronitrobenzene-degrading Nocardioides sp. strain PD653. Appl Environ Microbiol 75, 4452–4458.
- 23 Adak S & Begley TP (2019) Hexachlorobenzene catabolism involves a nucleophilic aromatic substitution and flavin-N5-oxide formation. *Biochemistry* 58, 1181– 1183.
- 24 Guo Y, Li D-F, Ji H, Zheng J & Zhou N-Y (2020) Hexachlorobenzene monooxygenase substrate selectivity and catalysis: structural and biochemical insights. *Appl Environ Microbiol* 87, e01965–20.
- 25 Adak S & Begley TP (2016) Dibenzothiophene catabolism proceeds via a flavin-N5-oxide intermediate. *J Am Chem Soc* **138**, 6424–6426.
- 26 Davoodi-Dehaghani F, Vosoughi M & Ziaee AA (2010) Biodesulfurization of dibenzothiophene by a newly

- isolated Rhodococcus erythropolis strain. *Bioresour Technol* **101**, 1102–1105.
- 27 Okai M, Lee WC, Guan L-J, Ohshiro T, Izumi Y & Tanokura M (2017) Crystal structure of dibenzothiophene sulfone monooxygenase BdsA from *Bacillus subtilis* WU-S2B. *Proteins* 85, 1171–1177.
- 28 Jun S-Y, Lewis KM, Youn B, Xun L & Kang C (2016) Structural and biochemical characterization of EDTA monooxygenase and its physical interaction with a partner flavin reductase. *Mol Microbiol* 100, 989–1003.
- 29 Armacost K, Musila J, Gathiaka S, Ellis HR & Acevedo O (2014) Exploring the catalytic mechanism of alkanesulfonate monooxygenase using molecular dynamics. *Biochemistry* 53, 3308–3317.
- 30 Niehaus TD, Folz J, McCarty DR, Cooper AJL, Moraga Amador D, Fiehn O & Hanson AD (2018) Identification of a metabolic disposal route for the oncometabolite S-(2-succino)cysteine in *Bacillus subtilis*. *J Biol Chem* **293**, 8255–8263.
- 31 Yang M, Soga T & Pollard PJ (2013) Oncometabolites: linking altered metabolism with cancer. *J Clin Invest* **123**, 3652–3658.
- 32 Zheng L, Cardaci S, Jerby L, MacKenzie ED, Sciacovelli M, Johnson TI, Gaude E, King A, Leach JDG, Edrada-Ebel R *et al.* (2015) Fumarate induces redox-dependent senescence by modifying glutathione metabolism. *Nat Commun* **6**, 6001.
- 33 Ternette N, Yang M, Laroyia M, Kitagawa M, O'Flaherty L, Wolhulter K, Igarashi K, Saito K, Kato K, Fischer R *et al.* (2013) Inhibition of mitochondrial aconitase by succination in fumarate hydratase deficiency. *Cell Rep* **3**, 689–700.
- 34 Piroli GG, Manuel AM, Walla MD, Jepson MJ, Brock JWC, Rajesh MP, Tanis RM, Cotham WE & Frizzell N (2014) Identification of protein succination as a novel modification of tubulin. *Biochem J* **462**, 231–245.
- 35 Frizzell N, Lima M & Baynes JW (2011) Succination of proteins in diabetes. *Free Radic Res* **45**, 101–109.
- 36 Blatnik M, Thorpe SR & Baynes JW (2008) Succination of proteins by fumarate: mechanism of inactivation of glyceraldehyde-3-phosphate dehydrogenase in diabetes. *Ann N Y Acad Sci* 1126, 272–275.
- 37 Spyrou G, Haggård-Ljungquist E, Krook M, Jörnvall H, Nilsson E & Reichard P (1991) Characterization of the flavin reductase gene (fre) of Escherichia coli and construction of a plasmid for overproduction of the enzyme. *J Bacteriol* **173**, 3673–3679.
- 38 Bajad SU, Lu W, Kimball EH, Yuan J, Peterson C & Rabinowitz JD (2006) Separation and quantitation of water soluble cellular metabolites by hydrophilic interaction chromatography-tandem mass spectrometry. *J Chromatogr A* **1125**, 76–88.

- 39 Santa T (2011) Derivatization reagents in liquid chromatography/electrospray ionization tandem mass spectrometry. *Biomed Chromatogr* 25, 1–10.
- 40 Thakur A, Somai S, Yue K, Ippolito N, Pagan D, Xiong J, Ellis HR & Acevedo O (2020) Substratedependent mobile loop conformational changes in alkanesulfonate monooxygenase from accelerated molecular dynamics. *Biochemistry* 59, 3582–3593.
- 41 Xiong J & Ellis HR (2012) Deletional studies to investigate the functional role of a dynamic loop region of alkanesulfonate monooxygenase. *Biochim Biophys* Acta 1824, 898–906.
- 42 Waterhouse A, Bertoni M, Bienert S, Studer G, Tauriello G, Gumienny R, Heer FT, de Beer TAP, Rempfer C, Bordoli L *et al.* (2018) SWISS-MODEL: homology modelling of protein structures and complexes. *Nucleic Acids Res* **46**, W296–W303.
- 43 Mukherjee T, Zhang Y, Abdelwahed S, Ealick SE & Begley TP (2010) Catalysis of a flavoenzyme-mediated amide hydrolysis. *J Am Chem Soc* **132**, 5550–5551.
- 44 Guedes IA, Barreto AMS, Marinho D, Krempser E, Kuenemann MA, Sperandio O, Dardenne LE & Miteva MA (2021) New machine learning and physics-based scoring functions for drug discovery. Sci Rep 11, 3198.
- 45 Santos KB, Guedes IA, Karl ALM & Dardenne LE (2020) Highly flexible ligand docking: benchmarking of the DockThor program on the LEADS-PEP proteinpeptide data set. J Chem Inf Model 60, 667–683.
- 46 Liew JJM, El Saudi IM, Nguyen SV, Wicht DK & Dowling DP (2021) Structures of the alkanesulfonate monooxygenase MsuD provide insight into C-S bond cleavage, substrate scope, and an unexpected role for the tetramer. *J Biol Chem* 297, 100823.
- 47 Yeh E, Cole LJ, Barr EW, Bollinger JM, Ballou DP & Walsh CT (2006) Flavin redox chemistry precedes substrate chlorination during the reaction of the flavin-dependent halogenase RebH. *Biochemistry* 45, 7904–7912.
- 48 Zhan X, Carpenter RA & Ellis HR (2008) Catalytic importance of the substrate binding order for the FMNH2-dependent alkanesulfonate monooxygenase enzyme. *Biochemistry* 47, 2221–2230.
- 49 Gao B & Ellis HR (2005) Altered mechanism of the alkanesulfonate FMN reductase with the monooxygenase enzyme. *Biochem Biophys Res Commun* 331, 1137–1145.

- 50 Chan C-M, Danchin A, Marlière P & Sekowska A (2014) Paralogous metabolism: S-alkyl-cysteine degradation in *Bacillus subtilis*. *Environ Microbiol* 16, 101–117.
- 51 Tan B, Lu Z, Dong S, Zhao G & Kuo M-S (2014) Derivatization of the tricarboxylic acid intermediates with O-benzylhydroxylamine for liquid chromatography-tandem mass spectrometry detection. *Anal Biochem* 465, 134–147.
- 52 Ellman GL (1959) Tissue sulfhydryl groups. *Arch Biochem Biophys* **82**, 70–77.
- 53 Bulaj G, Kortemme T & Goldenberg DP (1998) Ionization-reactivity relationships for cysteine thiols in polypeptides. *Biochemistry* **37**, 8965–8972.
- 54 Moran GR (2019) Anaerobic methods for the transientstate study of flavoproteins: the use of specialized glassware to define the concentration of dioxygen. *Methods Enzymol* **620**, 27–49.
- 55 Yoneda F, Sakuma Y, Ichiba M & Shinomura K (1976) Syntheses of isoalloxazines and isoalloxazine 5oxides. A new synthesis of riboflavin. *J Am Chem Soc* 98, 830–835.
- 56 Brosi R, Illarionov B, Heidinger L, Kim R-R, Fischer M, Weber S, Bacher A, Bittl R & Schleicher E (2020) Coupled methyl group rotation in FMN radicals revealed by selective deuterium labeling. *J Phys Chem B* 124, 1678–1690.

Supporting information

Additional supporting information may be found online in the Supporting Information section at the end of the article.

Fig. S1. SDS/PAGE and SEC analysis of YxeK wt and variants.

Fig. S2. Comparison of oxidative and nonoxidative reactions catalyzed by group C FPMOs.

Fig. S3-S8. NMR data from Fl_{N5O} synthesis.

Fig. S9. Comparison of the UV/Vis spectra of Fl_{N5O} and FMN.

Fig. S10. UPLC-HRMS analysis of malate conversion by YxeK-Fl_{N5O}.

Table S1. List of oligonucleotides used for construction of YxeK variants